First Amplitude Analysis of $B \to J/\psi \phi K$

Thomas Britton

Advisor:
Tomasz Skwarnicki

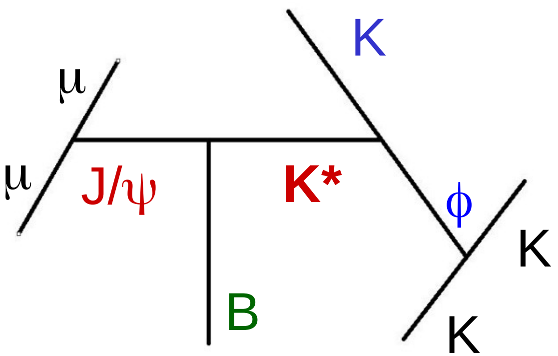

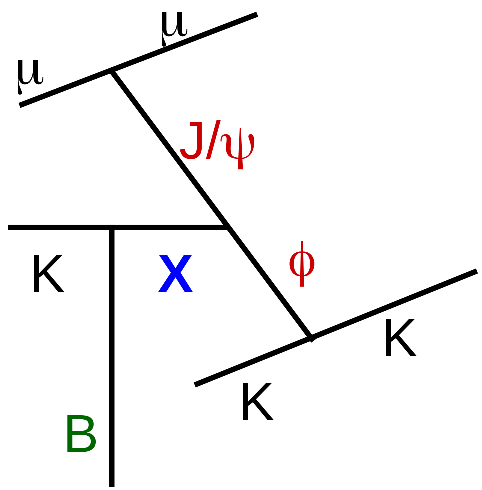

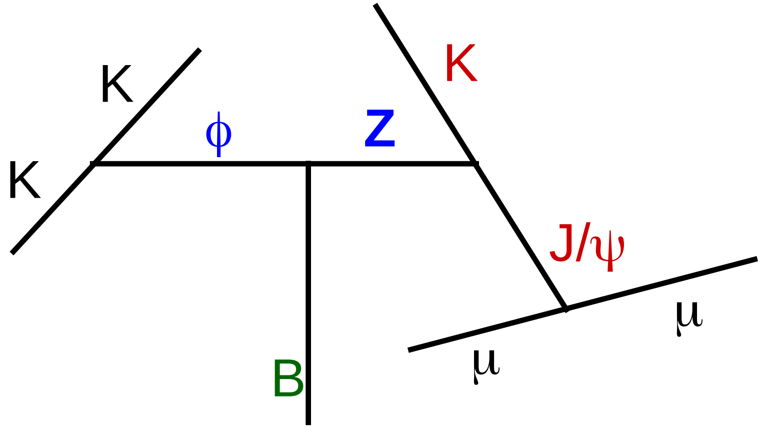

PRL 118, 022003
PRD 95, 012002

The LHCb experiment at CERN

- A tunnel 27 km (17 mi) in circumference on the border between France and Switzerland
- Home to the most powerful accelerator and 4 large experiments
  - **LHCb**
  - CMS
  - ATLAS
  - ALICE

The LHCb Detector at the LHC

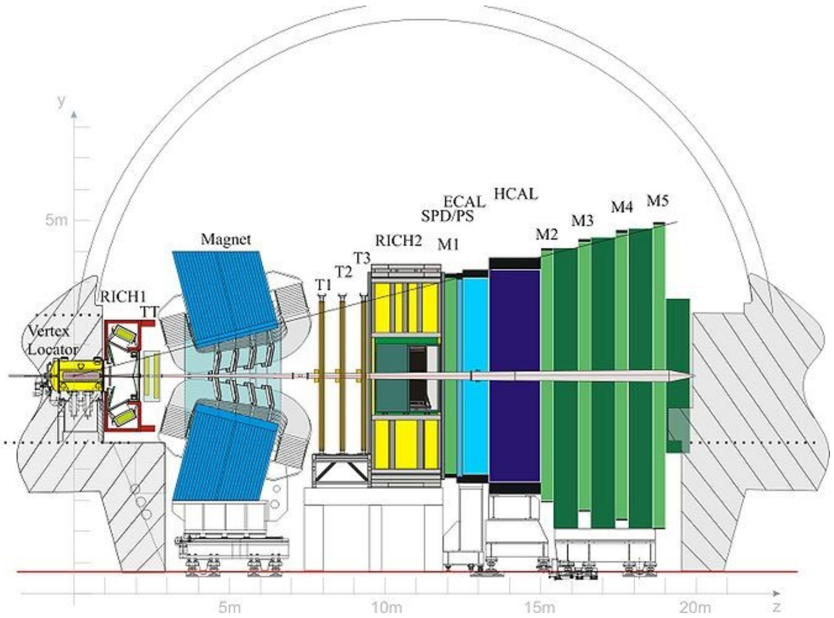

Int. J. Mod. Phys. A 30, 1530022 (2015)

- Single-arm forward spectrometer designed for precision measurements of CP violating decays, specifically decays involving bottom or charm hadrons
  - Covering $2<\eta<5$
- Great particle identification
  - Muons: ε ~97% with 1-3% of $\mu\rightarrow\pi$ misidentification
  - Kaons: ε ~95% with 5% of $\pi\rightarrow$K misidentification
- Good impact parameter resolution: $\sigma=20\mu$m
- Good momentum resolution: Δp/p=0.5% at 20GeV to 0.8% at 100GeV

Exotic hadrons at LHCb

- Over the last few years there has been exciting research in exotic spectroscopy, more specifically charmonium and bottomonium like states
- LHCb has contributed important results based on amplitude fits to the data:
  – Quantum number determination of X(3872) using $B^+ \rightarrow X(3872)K^+$, $X(3872) \rightarrow \rho^0 J/\psi$ decays
  – Study of the resonant nature of $Z(4430)^- \rightarrow \pi^- \psi'$ in $B^0 \rightarrow \psi' \pi^- K^+$ decays
  – Discovery of pentaquark candidates $P_c(4380)^+$ and $P_c(4450)^+ \rightarrow pJ/\psi$ in $\Lambda_b \rightarrow J/\psi p K^-$ decays
- My thesis focused on possible exotic $J/\psi\phi$ tetraquark contributions to $B \rightarrow J/\psi \phi K$ decays

X(3872)

Phys. Rev. Lett. 110, 222001 (2013)

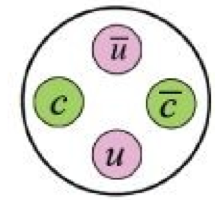

Z(4430)

PRL 112, 222002 (2014)
Phys. Rev. D 92, 112009 (2015)

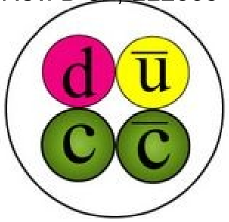

P_c

Phys. Rev. Lett. 115, 072001 (2015)

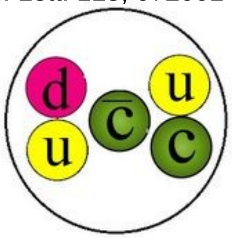

X(4140)?

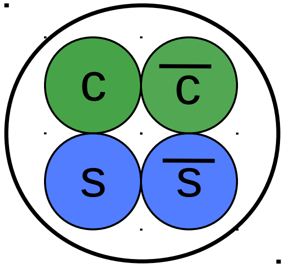

B → J/ψϕK at CDF

CDF arXiv:1101.6058
2011 unpublished update

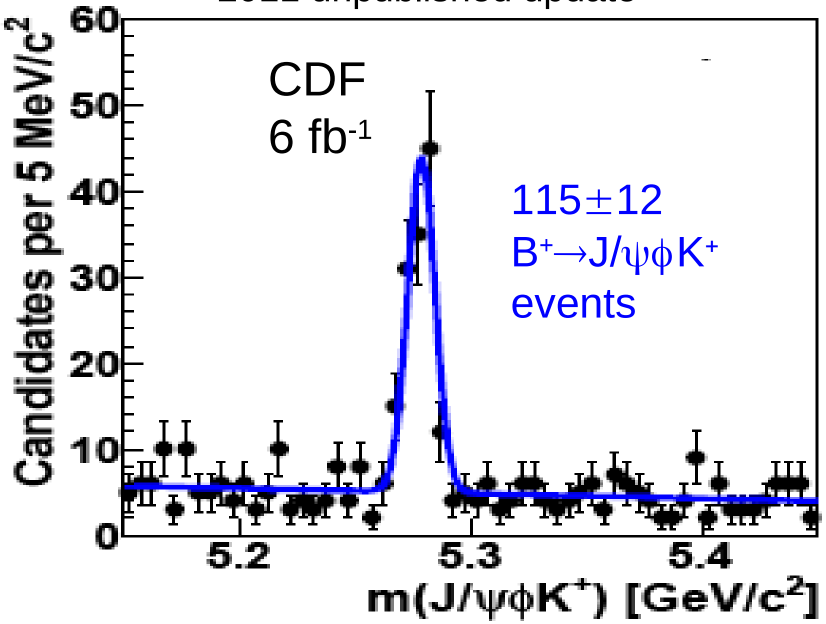

4143±3±1 MeV
Γ=15±10 MeV

Prior analysis 2009: 2.7 fb-1
Phys.Rev.Lett.102:242002,2009

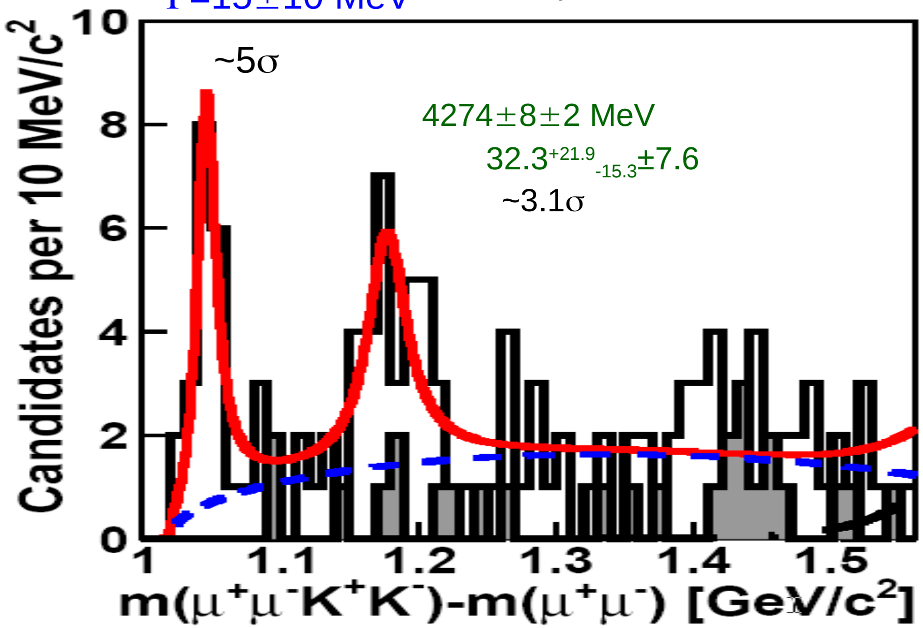

- Narrow near-threshold X(4140) peak. Possibly also a second peak at 4274 MeV.
- They did not investigate the high J/ψϕ mass region due to high backgrounds.

$B \rightarrow J/\psi\phi K$ at LHCb (Early Results)

Phys. Rev. D 85, 091103(R) (2012)

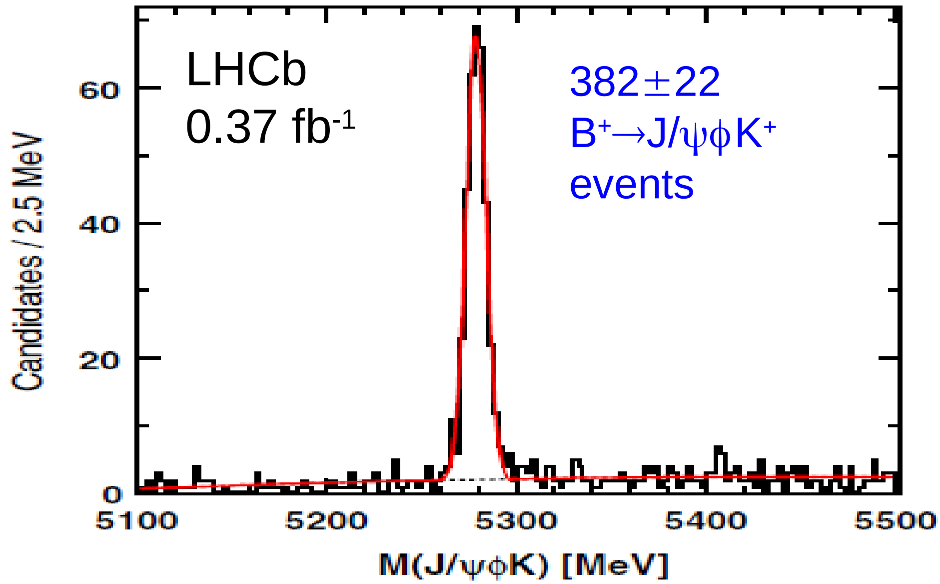

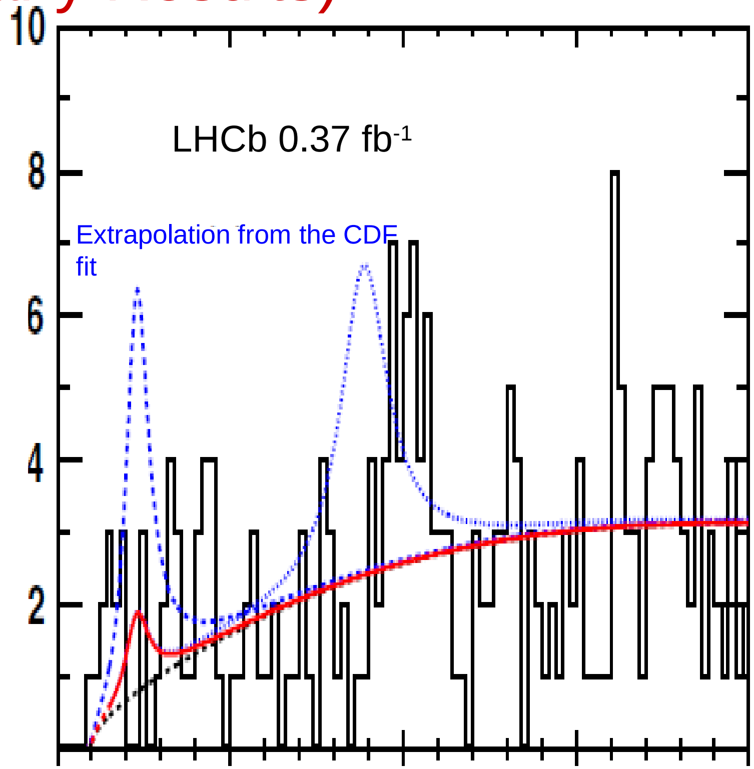

X(4140)
2.4σ tension
With CDF

- In 2012 LHCb looked at 0.37 fb^{-1} of data with about double the number $B \rightarrow J/\psi\phi K$ events compared to CDF
- Saw no evidence for a narrow X(4140) (2.4σ tension with CDF)

$B \to J/\psi\phi K$ at CMS

Phys. Lett. B 734 (2014) 261

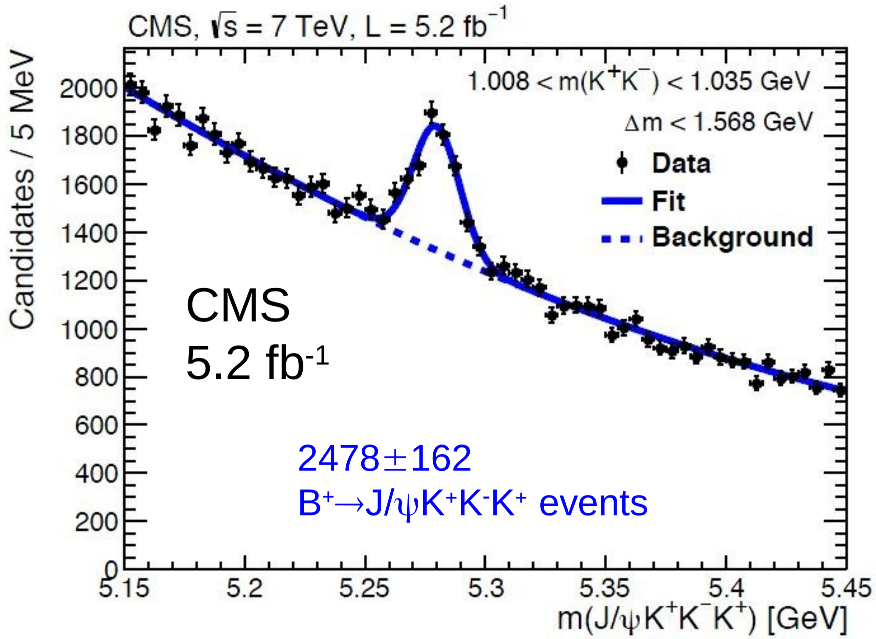

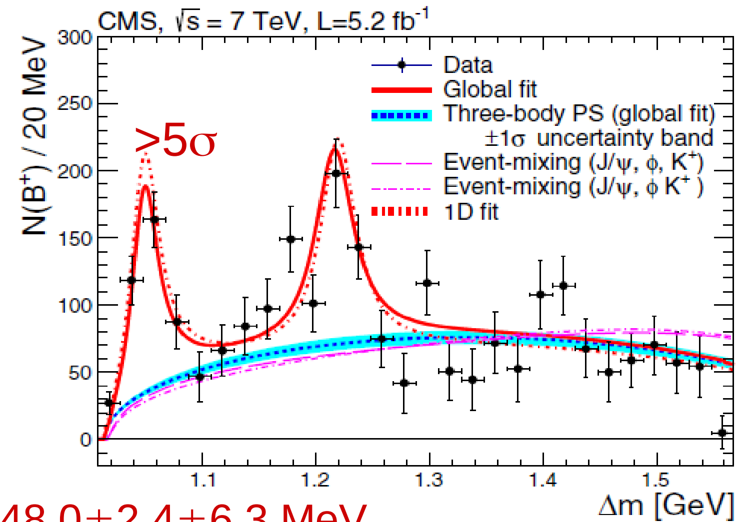

4148.0±2.4±6.3 MeV

Γ=28$^{+15}_{-11}$(stat)±19(syst)MeV

4313.8±5.3±7.3 MeV

3.2σ different from CDF!

- In 2013 CMS analyzed 5.2 fb^{-1} of data and obtained, at the time, the largest $B \to J/\psi\phi K$ sample analyzed but with high backgrounds.
- They confirmed X(4140) with somewhat larger width.
- They did not quote significance for the second peak and saw it at 3.2σ higher mass than CDF
- Once again the high $J/\psi\phi$ mass region was not analyzed

$B \to J/\psi \phi K$ at D0

Phys. Rev. D 89, 012004 (2014)

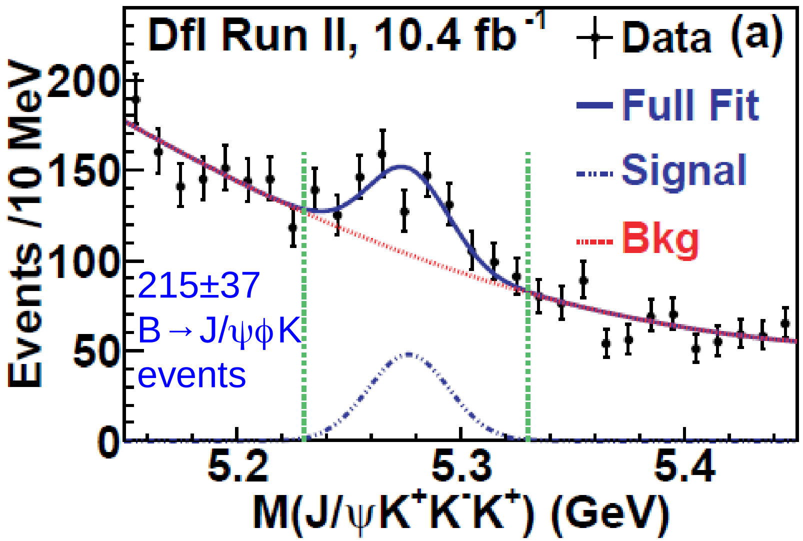

M=4159.0±4.3±6.6 MeV

Γ=19.9±12.6$^{+1}_{-8}$ MeV

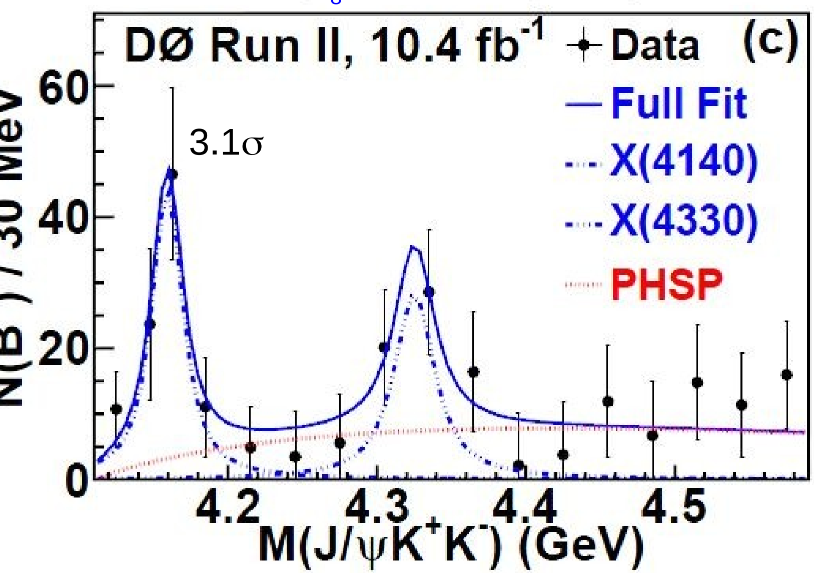

- Also in 2013 D0 looked at 10.4 fb^{-1} of data and saw 3.1σ evidence for X(4140) as well. The 2nd peak is not significant.
- In 2015 D0 claimed observation of prompt X(4140) productions in $p\bar{p}$ collisions (4.7σ) Phys.Rev.Lett. 115 (2015) 232001

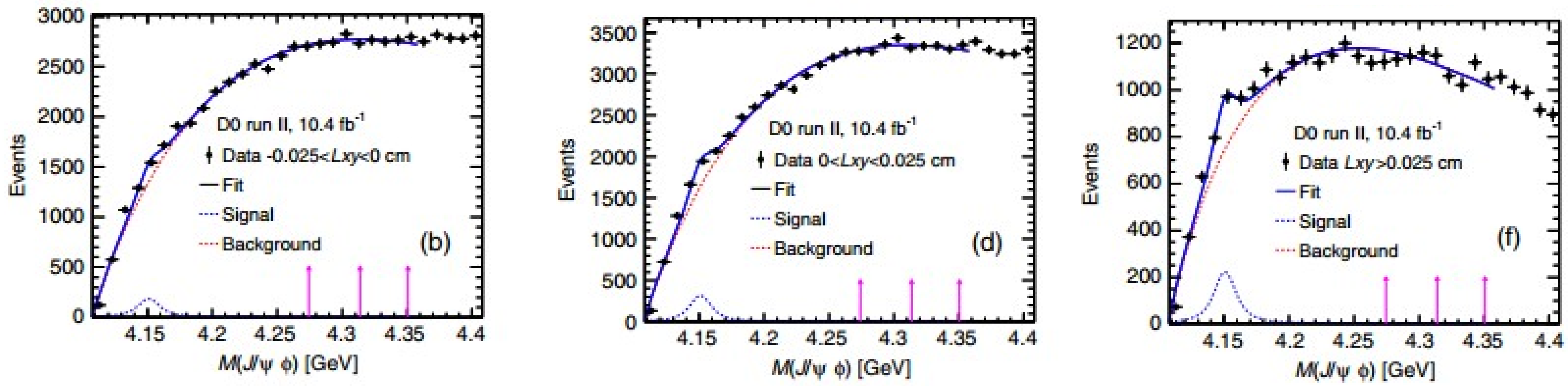

B→J/ψϕK at Belle & Babar

AIP Conference Proceedings 1257, 189 (2010);

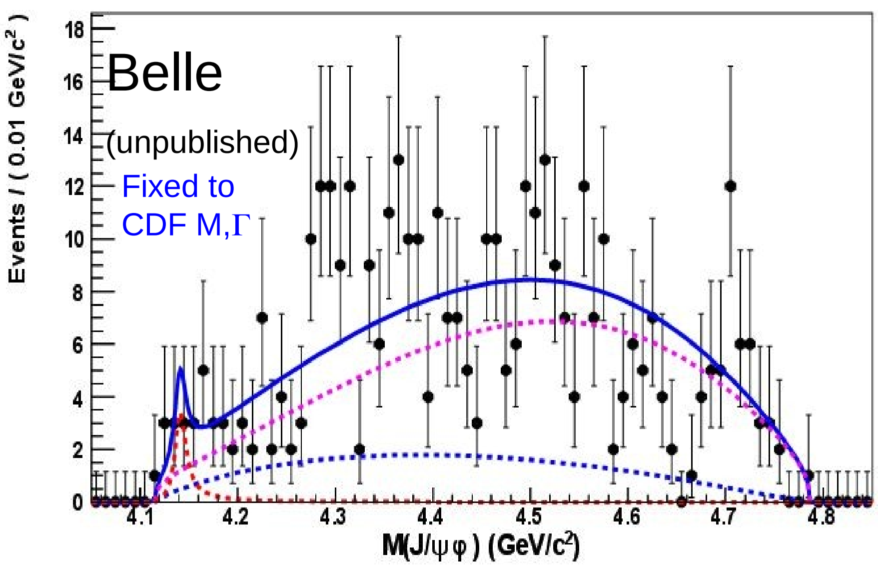

Phys. Rev. D91 (2015), no. 1 012003

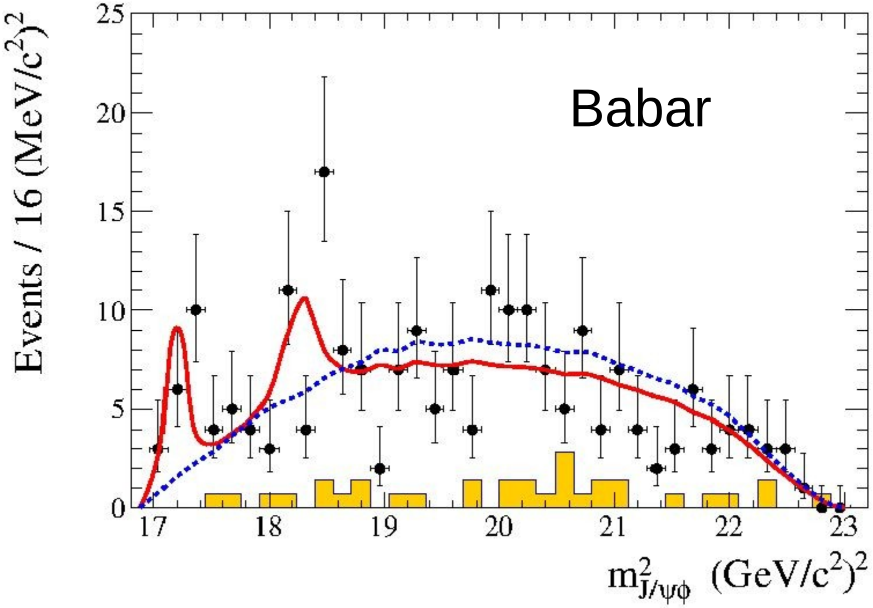

- Both Belle and Babar also looked at B→J/ψϕK in 2010 and 2014, respectively.
- Low backgrounds for B mesons produced at Y(4S) at the e^+e^- colliders
- They studied entire J/ψϕ mass region but suffered from low statistics, especially at low masses due to poor threshold efficiency.
- Belle analyzed 325±21 B→J/ψϕK events and found no evidence for X(4140)
- Babar, only having 215 B→J/ψϕK events, found little evidence for either state (<2σ significance)
- Neither in contradiction with the results from the hadron colliders

Data selection details

The data for this analysis was selected similarly to the first analysis by LHCb (PRD 85, 091103).

Cuts were re-optimized and were about 50% more efficient, though with the compromise of higher background levels.

Particle	Quantity	Requirement
All tracks	Track quality: χ^2/ndf	< 4
All tracks(2012)	GhostProb.	< 0.47
All tracks	Clone	Default
μ	p_T	> 550 MeV
μ	IsMuon	True
μ	PID_μ (DLL(μ-π))	> 0
Di-μ	Vertex quality: χ^2/ndf	< 9
Di-μ	p_T	> 1.5 GeV
J/ψ	$m_{\mu^+ \mu m}$ window	[3.040,3.140] GeV
K	PID_K (DLL(K-π))	> 0
K	p_T	> 250 MeV
K	χ^2_{IP}	> 9
ϕ	$\lvert m_{K^+K^-} - M_\phi \rvert$	< 15 MeV
ϕ	# of ϕ candidates	$= 1$
B	$m_{J/\psi \phi K^+}$ window	[5.10, 5.5] GeV
B	Vertex quality: χ^2/ndf	< 9
B	p_T	> 2.0 GeV
B	Lifetime: τ	> 0.25 ps
B	Trigger	L0, Hlt1, Hlt2 TOS (see text)
B	DLL	< 5

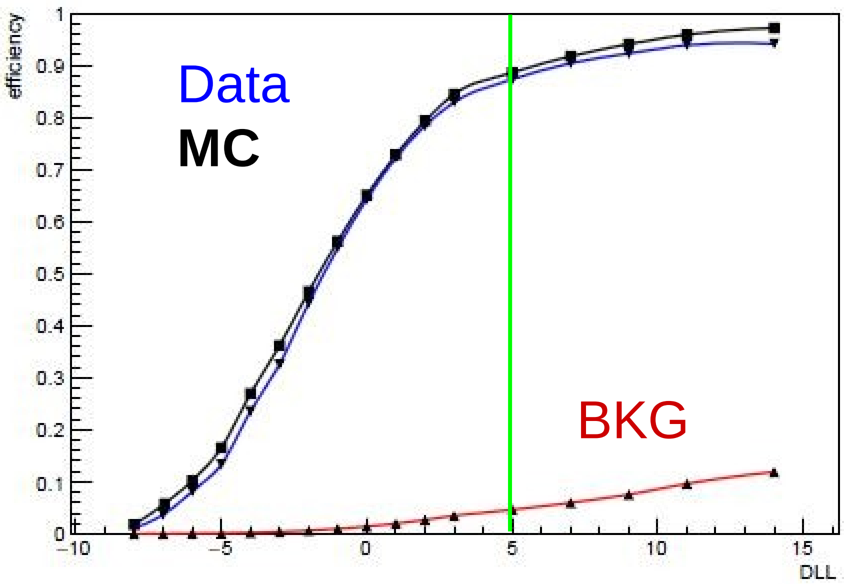

Data set

- Analysis performed on ~3 fb^{-1} of data collected by LHCb in 2011 and 2012.
- $J/\psi\phi K$ combinations were taken with only one ϕ candidate in $K^+K^-K^+$
  - Yields **4289±151** $B\rightarrow J/\psi\phi K$ events and a background fraction of **β=23±6%** in the 5270-5290 MeV region (used in the amplitude fits)
- This amounts to a larger $B\rightarrow J/\psi\phi K$ sample than any previously published analysis

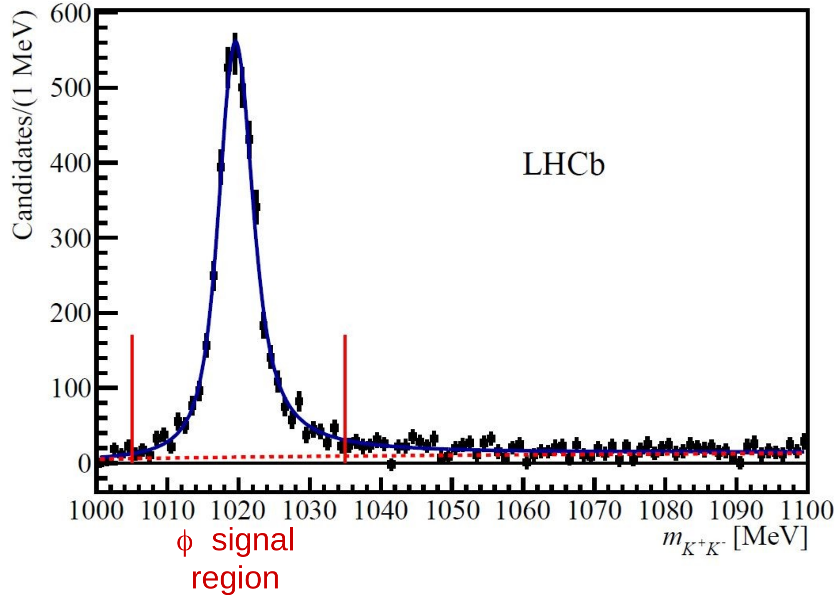

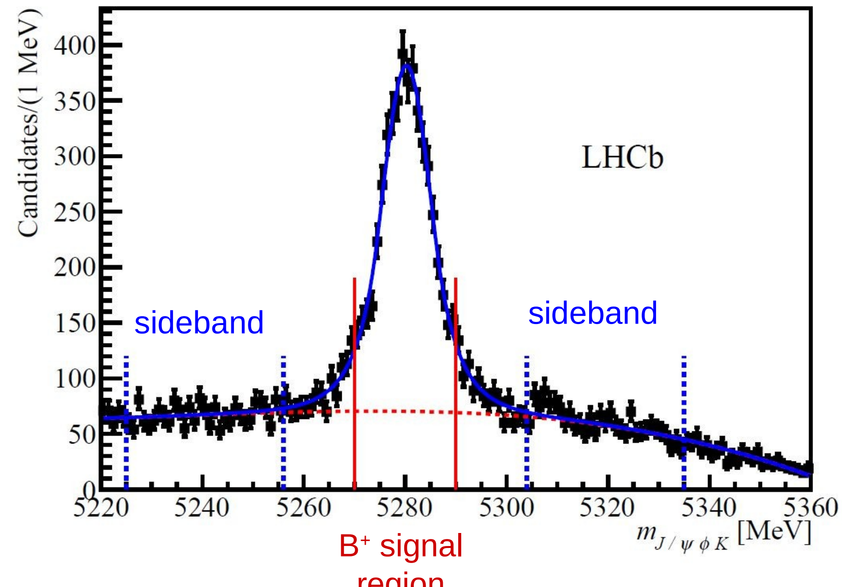

Amplitude fit analysis

- Prior analyses used naive 1D mass fits with ad-hoc background shapes
  - Amplitude analysis needed to investigate the origin of any $J/\psi\phi$ structures and determine the quantum numbers of any states seen (important for their interpretation)
  - Analysis of J/ψ and ϕ polarizations greatly increases the sensitivity of this analysis as opposed to the Dalitz plot alone
- Difficulties:
  - Two spin-1 particles involved, both decaying:
    - $J/\psi \rightarrow \mu^+\mu^-$, $\phi \rightarrow K^+K^-$
  - Three different decay chains which can interfere
    - $B \rightarrow X K$ with $X \rightarrow J/\psi\ \phi$
    - $B \rightarrow J/\psi\ K^*$, $K^* \rightarrow \phi K$
    - $B \rightarrow Z \phi$ with $Z \rightarrow J/\psi\ K$
  - Highly excited K* states are not well understood experimentally
  - Phase-space is 6-dimensional:
    - E.g. for K* decay chain in helicity formulation: $\mathbf{m}_{\phi K}$, $\cos(\theta_{K^*})$, $\cos(\theta_\psi)$, $\cos(\theta_\phi)$, $\Delta\phi_{K^*,\psi}$, $\Delta\phi_{K^*,\phi}$
- Use the same fit formalism as in Z(4430) analysis:
  - unbinned 6D maximum likelihood fit
  - cFit for background subtraction (issues with fit stability in sFit)
  - exact 6D treatment of efficiency corrections for the signal part (no parameterization needed)
  - use helicity formalism to write down decay amplitudes

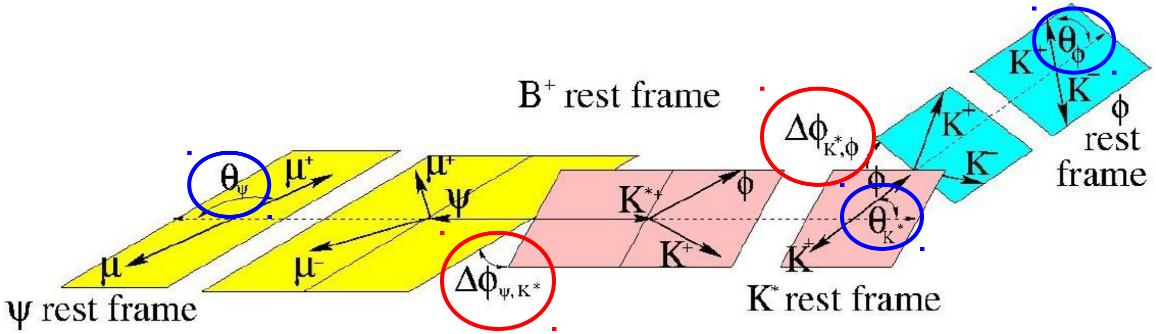

Diagram of the 5 angular variables for the K* decay chain

Computing the angles (an example)

For a particle P produced in a two body decay A→PB and decaying to two particles P→CD. With the momentum in the rest frame of P

sibling daughter

$$\cos\theta_P = -\frac{\vec{p}_B \cdot \vec{p}_C}{|\vec{p}_B|\,|\vec{p}_C|},$$

The inter-planar angle is found analogously to that of $\Delta\phi_{K^*,J/\psi}$

In this case the momenta are in the rest frame of B

$$\Delta\phi_{K^*,J/\psi} = \text{atan2}(\sin\Delta\phi_{K^*,J/\psi}\;,\;\cos\Delta\phi_{K^*,J/\psi})$$

$$\cos\Delta\phi_{K^*,J/\psi} = \frac{\vec{a}_{K^+}\cdot\vec{a}_{\mu^+}}{|\vec{a}_{K^+}|\,|\vec{a}_{\mu^+}|}$$

$$\sin\Delta\phi_{K^*,J/\psi} = \frac{[\vec{p}_{J/\psi}\times\vec{a}_{K^+}]\cdot\vec{a}_{\mu^+}}{|\vec{p}_{J/\psi}|\,|\vec{a}_{K^+}|\,|\vec{a}_{\mu^+}|}$$

$$\vec{a}_{K^+} = \vec{p}_{K^+} - \frac{\vec{p}_{K^+}\cdot\vec{p}_{K^{*+}}}{|\vec{p}_{K^{*+}}|^2}\,\vec{p}_{K^{*+}}$$

$$\vec{a}_{\mu^+} = \vec{p}_{\mu^+} - \frac{\vec{p}_{\mu^+}\cdot\vec{p}_{J/\psi}}{|\vec{p}_{J/\psi}|^2}\,\vec{p}_{J/\psi}\,,$$

Matrix element

- Each decay chain (K*,X,Z) requires its own unique matrix element with summing over j states belonging to the chain:

Mass dependence (BW amplitude or constant for NR)

Complex helicity couplings

$$\mathcal{M}^{K^*}_{\Delta\lambda_\mu} \equiv \sum_j R(m_{\phi K}|M_{0\,K^*\,j},\Gamma_{0\,K^*\,j}) \sum_{\lambda_{J/\psi}=-1,0,1}\ \sum_{\lambda_\phi=-1,0,1} A^{B\to J/\psi\,K^*\,j}_{\lambda_{J/\psi}}\, A^{K^*\to\phi K\,j}_{\lambda_\phi}$$

Angular distribution

$$d^{J_{K^*\,j}}_{\lambda_{J/\psi},\lambda_\phi}(\theta_{K^*})\, d^1_{\lambda_\phi,0}(\theta_\phi)\, e^{i\lambda_\phi \Delta\phi_{K^*,\phi}}\, d^1_{\lambda_{J/\psi},\Delta\lambda_\mu}(\theta_{J/\psi})\, e^{i\lambda_{J/\psi}\Delta\phi_{K^*,J/\psi}}$$

$$\mathcal{M}^{X}_{\Delta\lambda_\mu} \equiv \sum_j R(m_{J/\psi\,\phi}|M_{0\,X\,j},\Gamma_{0\,X\,j}) \sum_{\lambda_{J/\psi}=-1,0,1}\ \sum_{\lambda_\phi=-1,0,1} A^{X\to J/\psi\,\phi\,j}_{\lambda_{J/\psi},\lambda_\phi}$$

$$d^{J_X\,j}_{0,\lambda_{J/\psi}-\lambda_\phi}(\theta_X)\, d^1_{\lambda_\phi,0}(\theta^X_\phi)\, e^{i\lambda_\phi \Delta\phi_{X,\phi}}\, d^1_{\lambda_{J/\psi},\Delta\lambda_\mu}(\theta^X_{J/\psi})\, e^{i\lambda_{J/\psi}\Delta\phi_{X,J/\psi}}$$

$$\mathcal{M}^{Z}_{\Delta\lambda_\mu} \equiv \sum_j R(m_{J/\psi\,K}|m_{0\,Z\,j},\Gamma_{0\,Z\,j_Z}) \sum_{\lambda_{J/\psi}=-1,0,1}\ \sum_{\lambda_\phi=-1,0,1} A^{B\to Z\phi\,j}_{\lambda_\phi}\, A^{Z\to J/\psi\,K\,j}_{\lambda_{J/\psi}}$$

$$d^{J_Z\,j}_{\lambda_{J/\psi},\lambda_{J/\psi}}(\theta_Z)\, d^1_{\lambda_\phi,0}(\theta^Z_\phi)\, e^{i\lambda_\phi \Delta\phi_{Z,\phi}}\, d^1_{\lambda_{J/\psi},\Delta\lambda_\mu}(\theta^Z_{J/\psi})\, e^{i\lambda_{J/\psi}\Delta\phi_{K^*,J/\psi}}$$

$$|\mathcal{M}^{K^*+X+Z}|^2 = \sum_{\Delta\lambda_\mu=\pm1} \left| \mathcal{M}^{K^*}_{\Delta\lambda_\mu} + e^{i\alpha^X \Delta\lambda_\mu}\mathcal{M}^{X}_{\Delta\lambda_\mu} + e^{i\alpha^Z \Delta\lambda_\mu}\mathcal{M}^{Z}_{\Delta\lambda_\mu} \right|^2$$

LS Amplitudes

- In general, for strong decays, such as K*→ϕK we require:

$$A^{A\to B\,C}_{-\lambda_B,-\lambda_C} = P_A\,P_B\,P_C\,(-1)^{J_B+J_C-J_A}\,A^{A\to B\,C}_{\lambda_B,\,\lambda_C}$$

- It is helpful to not fit these helicity couplings directly but instead fit an equivalent number of independent LS couplings (B_{LS}) where L is the orbital angular momentum in the decay and S is total spin of the daughter particles. The relation uses the Clebsch-Gordan coefficients and is given by

$$A^{A\to B\,C}_{\lambda_B,\lambda_C} = \sum_L \sum_S \sqrt{\frac{2L+1}{2J_A+1}}\,B_{L,S}\left(\begin{array}{cc|c} J_B & J_C & S \\ \lambda_B & -\lambda_C & \lambda_B-\lambda_C \end{array}\right)\left(\begin{array}{cc|c} L & S & J_A \\ 0 & \lambda_B-\lambda_C & \lambda_B-\lambda_C \end{array}\right)$$

Number of free parameters

Note: The mass and width are always free parameters and included in the count below

J^P \ Decay chain	K*	X	Z
0^+	Forbidden (parity)	6	Forbidden (parity)
0^-	4	4	4
1^+	10	8	10
1^-	8	10	8
2^+	8	12	8
2^-	10	10	10

Background parameterization

- Took the same approach as used in the Z(4430) and pentaquark analyses:
  - Use B+ mass sidebands to parameterize background in the fitted sample
  - For technical reasons need to add background PDF to the matrix element squared, thus it must be divided by parameterized efficiency

$$-\ln L(\overrightarrow{\omega}) = -\Sigma_i \ln\left[|\mathcal{M}(m_{\phi K\ i}, \Omega_i|\overrightarrow{\omega})|^2 + \frac{\beta\, I(\overrightarrow{\omega})}{(1-\beta) I_{\rm bkg}} \frac{\mathcal{P}^u_{\rm bkg}(m_{\phi K\ i}, \Omega_i)}{\Phi(m_{\phi K\ i})\epsilon(m_{\phi K\ i}, \Omega_i)}\right]$$

  - Assume that both 6D functions used in the background parameterization factorize to a product of 2D functions:

$$\frac{\mathcal{P}^u_{\rm bkg}(m_{\phi K}, \Omega)}{\Phi(m_{\phi K})} = P_{{\rm bkg}_1}(m_{\phi K}, \cos\theta_{K^*}) \cdot P_{{\rm bkg}_2}(\cos\theta_\phi | m_{\phi K})$$
$$\cdot P_{{\rm bkg}_3}(\cos\theta_{J/\psi}|m_{\phi K}) \cdot P_{{\rm bkg}_4}(\Delta\phi_{K^*,\phi}|m_{\phi K}) \cdot P_{{\rm bkg}_5}(\Delta\phi_{K^*,J/\psi}|m_{\phi K})$$
$$\epsilon(m_{\phi K}, \Omega) = \epsilon_1(m_{\phi K}, \cos\theta_{K^*}) \cdot \epsilon_2(\cos\theta_\phi|m_{\phi K})$$
$$\cdot\epsilon_3(\cos\theta_{J/\psi}|m_{\phi K}) \cdot \epsilon_4(\Delta\phi_{K^*,\phi}|m_{\phi K}) \cdot \epsilon_5(\Delta\phi_{K^*,J/\psi}|m_{\phi K})$$

  - All 2D functions obtained by smoothed 2D histograms of sidebands and signal MC events, respectively.

Background and Efficiency Parameterization

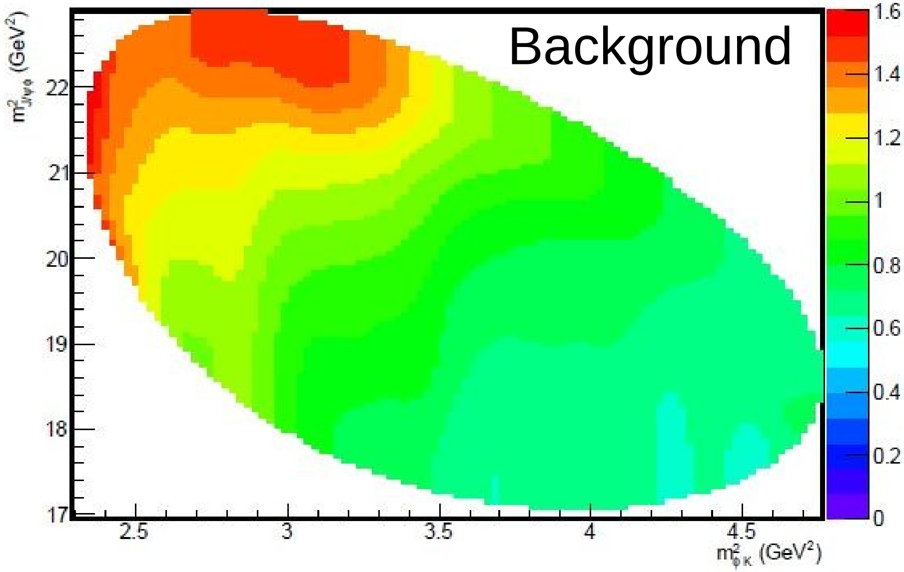

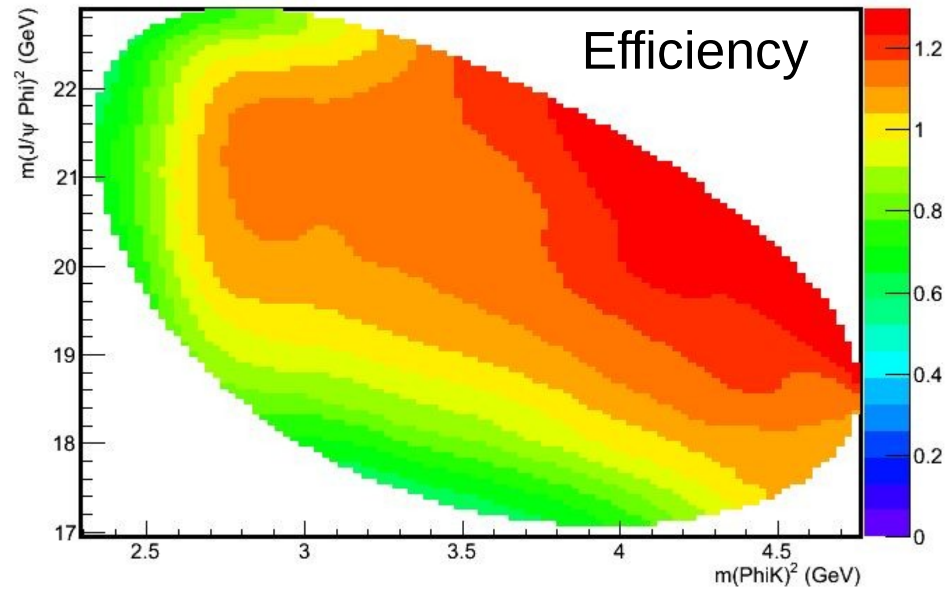

(The normalization arbitrarily corresponds to an average efficiency of 1 over phase-space.)

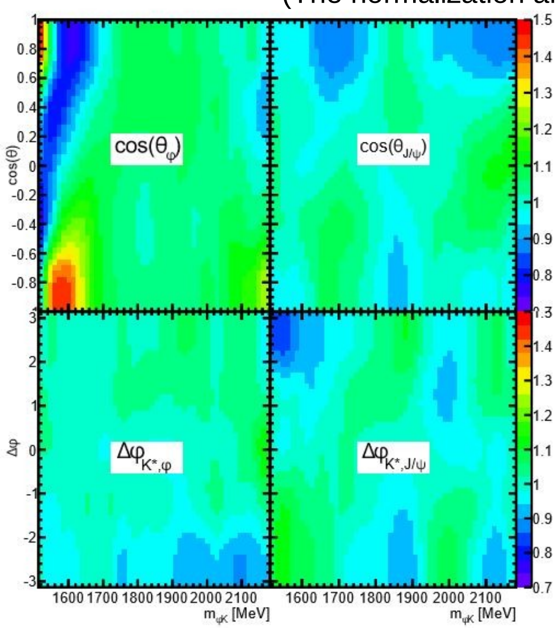

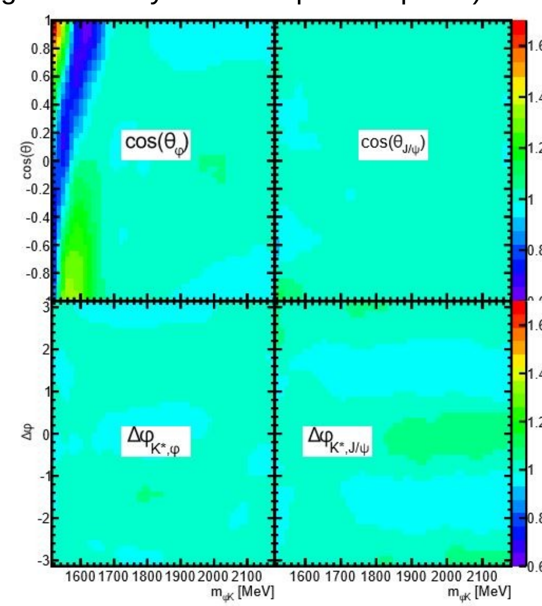

Data

Background-subtracted and efficiency-corrected

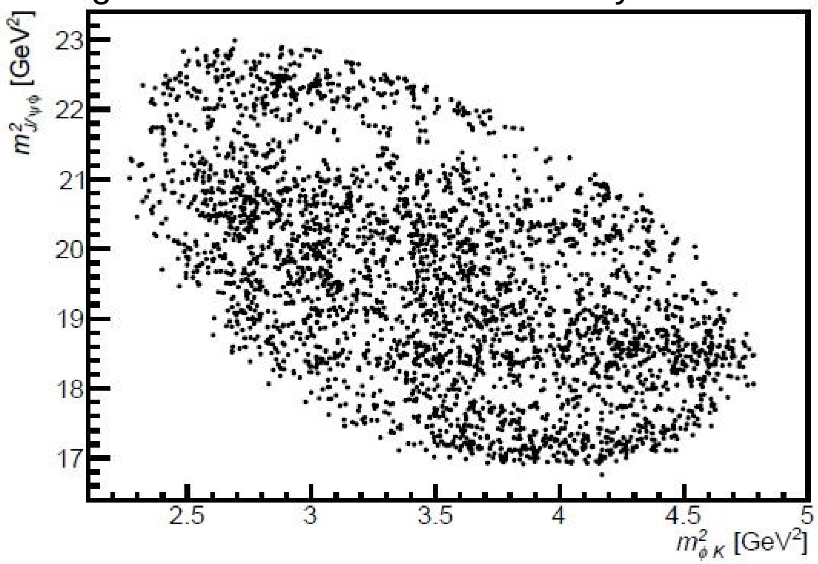

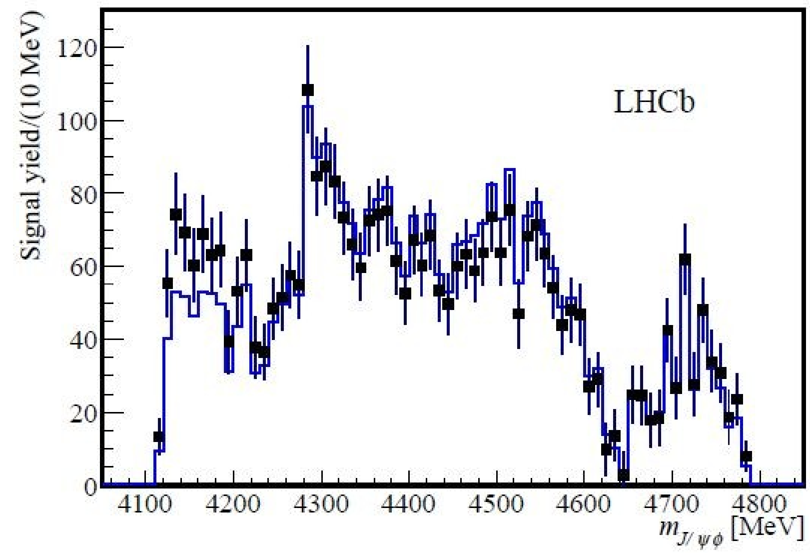

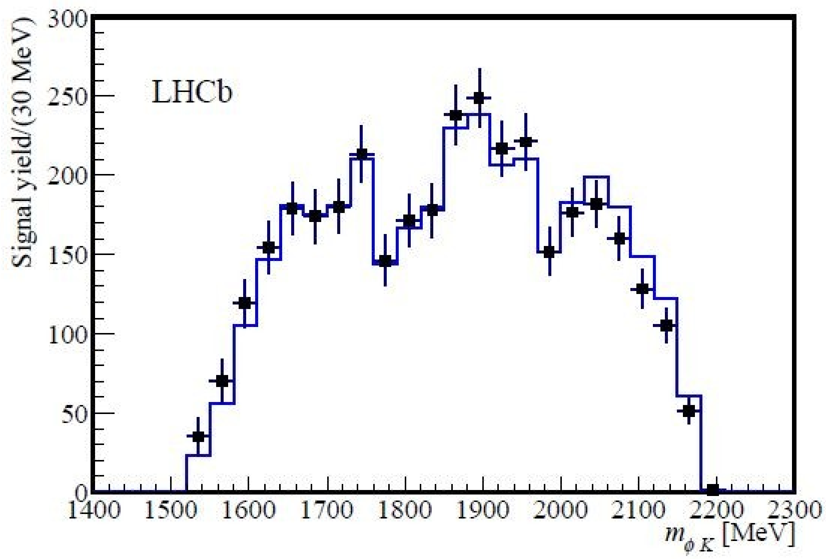

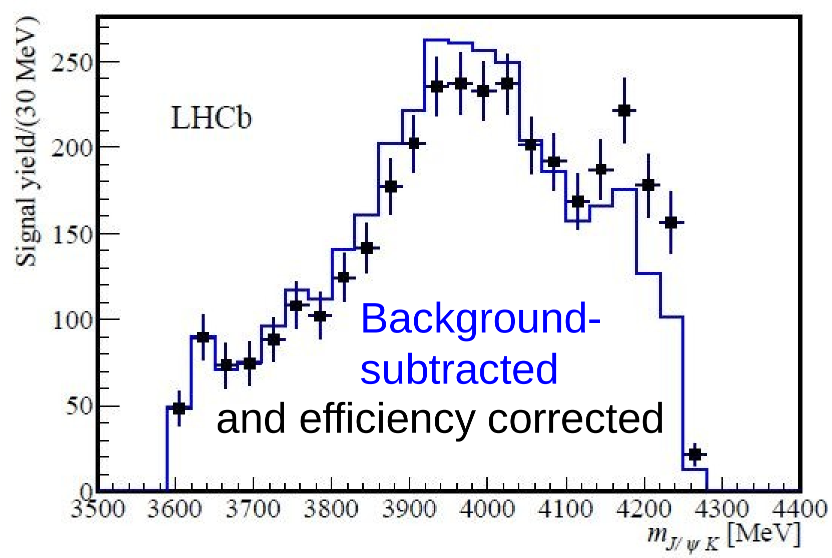

Comparison of CMS/LHCb data

Efficiency corrected and background subtracted.

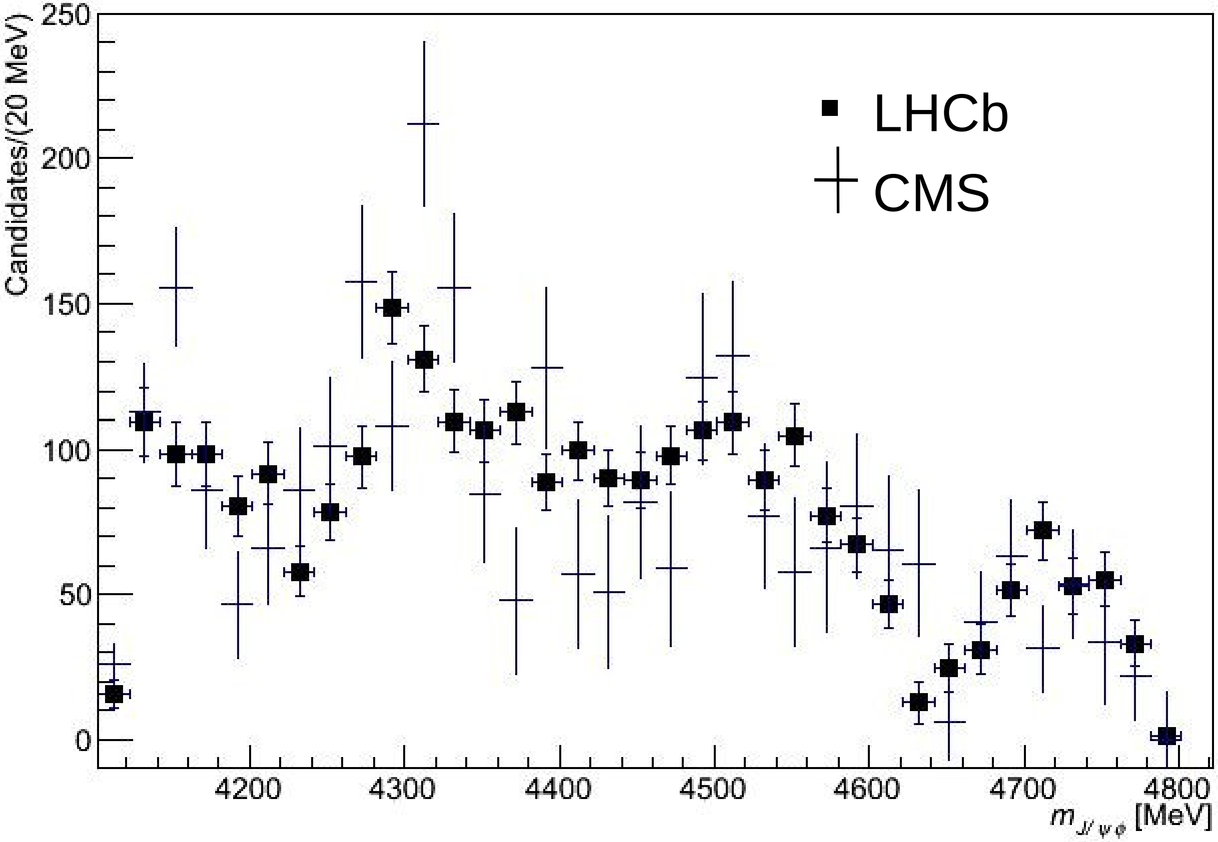

K* Model

- All K* states (except 0^{++}) between kinematic boundaries are allowed to decay to ϕK but may not have been seen in experiment because previous searches are typically old scattering experiments with low statistics at high masses

- All known excited states are broad: Γ~150-400 MeV

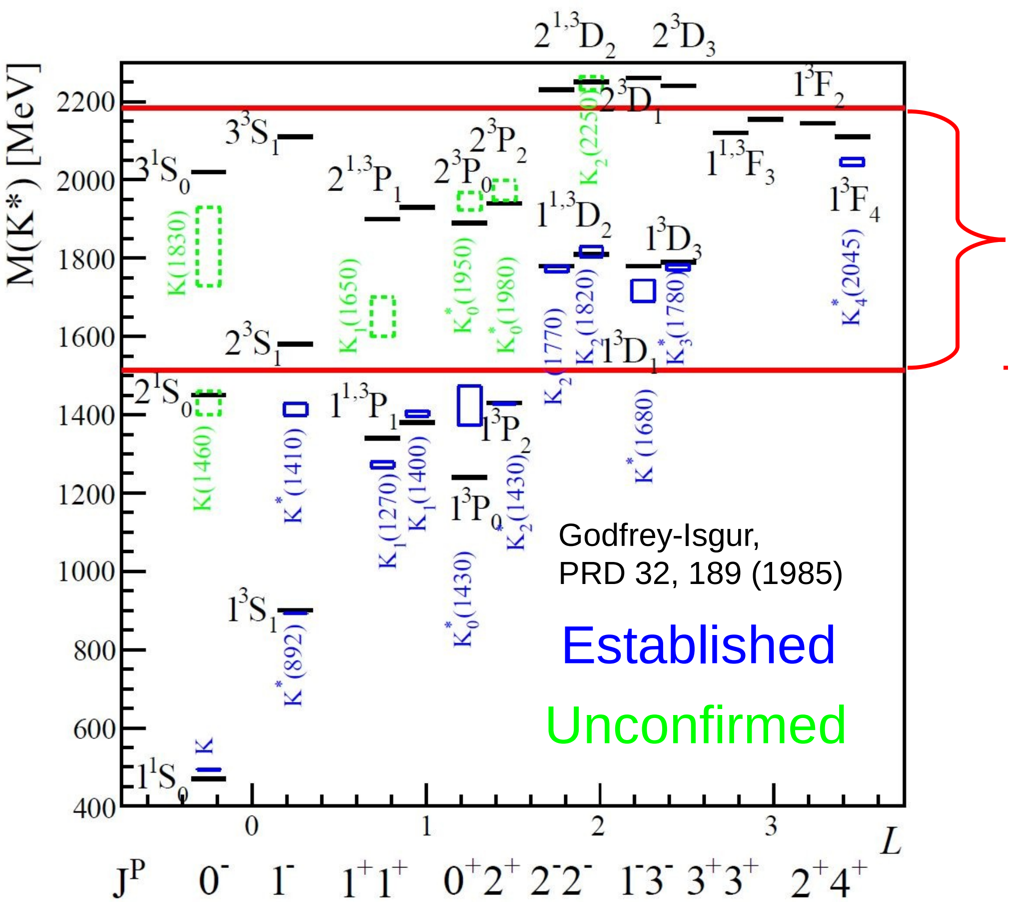

- Guidance from quark model was used to inform choices for K* sector
- Try a multitude of predicted K* states (both known and unknown)
- No constraints placed on mass or width parameters (**fits don't depend on predictions or previous measurements**)
- Take K* contributions greater than ~2σ significance.

K* only model

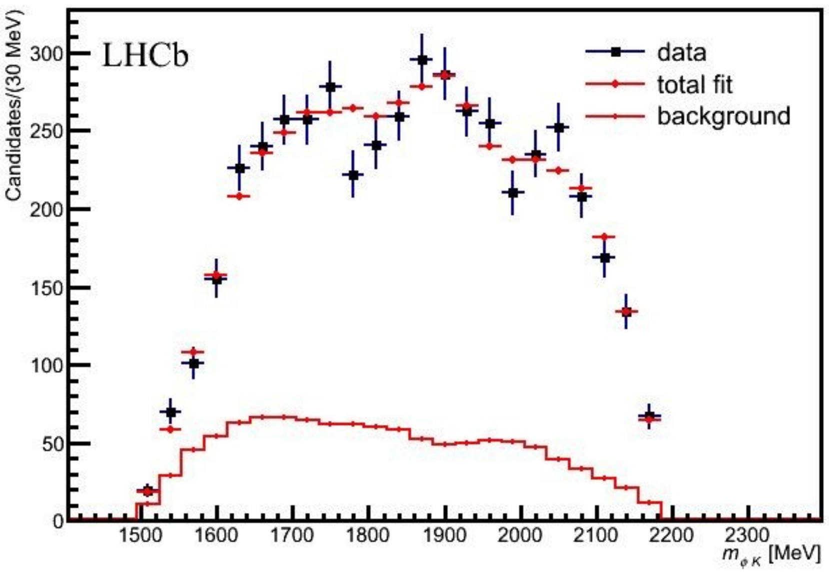

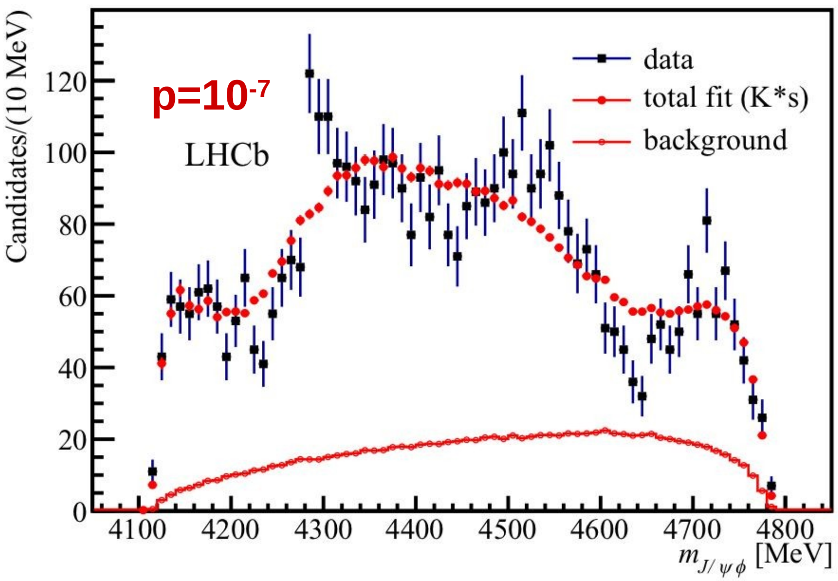

- Fits without exotic contributions (X,Z) were tried:
  - Example: two $2P_{1+}$, two $2D_{1-}$, and one of 1^3F_{3+}, 1^3D_{1-}, 3^3S_{1-}, 3^1S_{0-}, 2^3P_{2+}, 1^3F_{2+}, 1^3D_{3-}, 1^3F_{4+}. Contained 104 free parameters.

- Further K* additions, including states not predicted by the quark model, does not change the conclusion that non-K* contributions are needed to adequately describe all distributions

Default model

- We next considered adding possible exotic X and Z^+ states as well as removing insignificant or implausible K* states leading us to a default model
- Only X states give very significant improvements in fit qualities
- We now introduce the default model which resulted from the inclusion of X states and pruning of the K* model.

Default fit plots

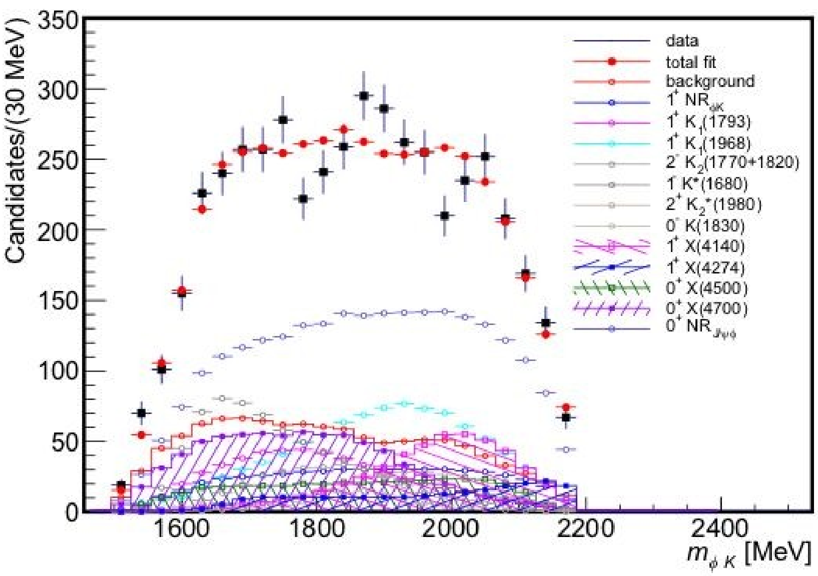

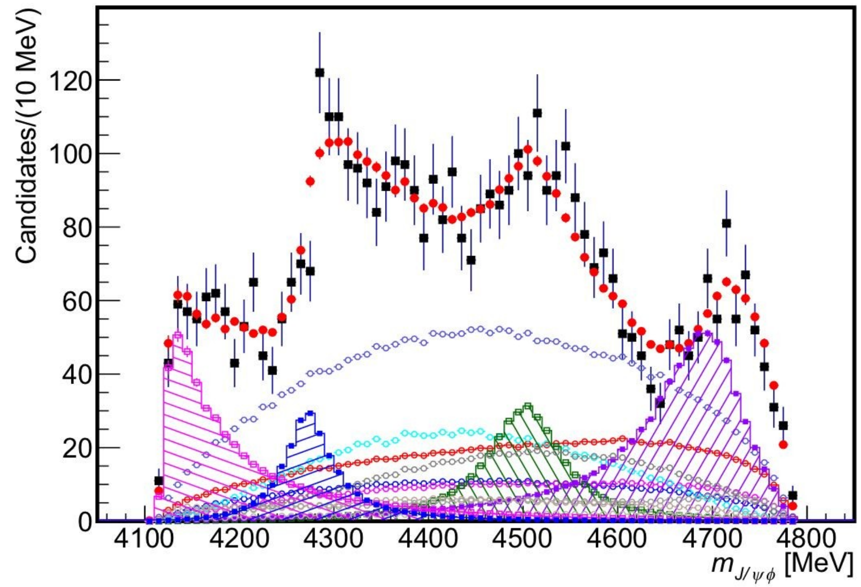

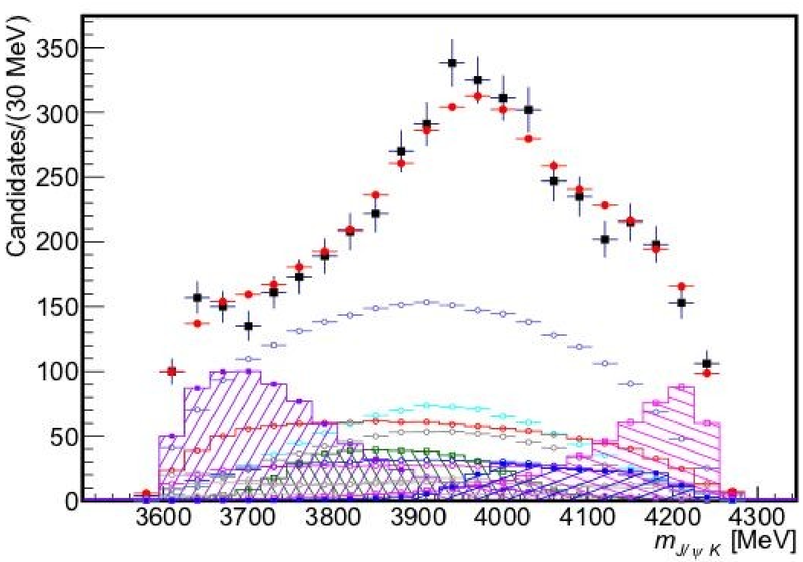

- 98 Free parameters
- 1D $J/\psi\phi$ p-value: 22%
- 2D Dalitz plane with adaptive binning χ^2= 438.7/496 (17%)
- 6D with adaptive binning χ^2 =462.9/501 (2.3%)

K* angles

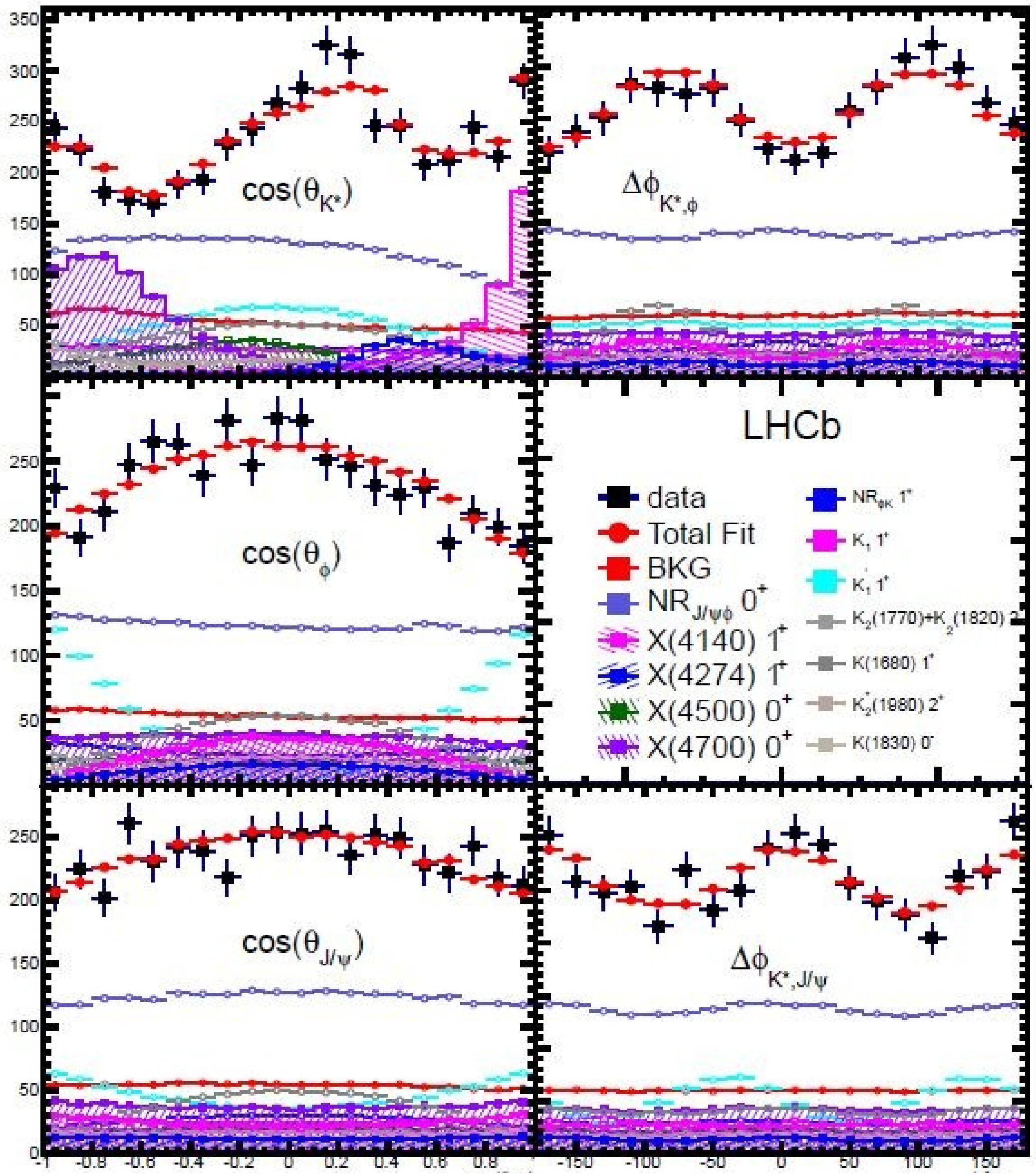
cos(θK*)
ΔφK*,φ
cos(θφ)
cos(θJ/ψ)
ΔφK*,J/ψ
LHCb
data
Total Fit
BKG
NRJ/ψφ 0+
X(4140) 1+
X(4274) 1+
X(4500) 0+
X(4700) 0+

X angles

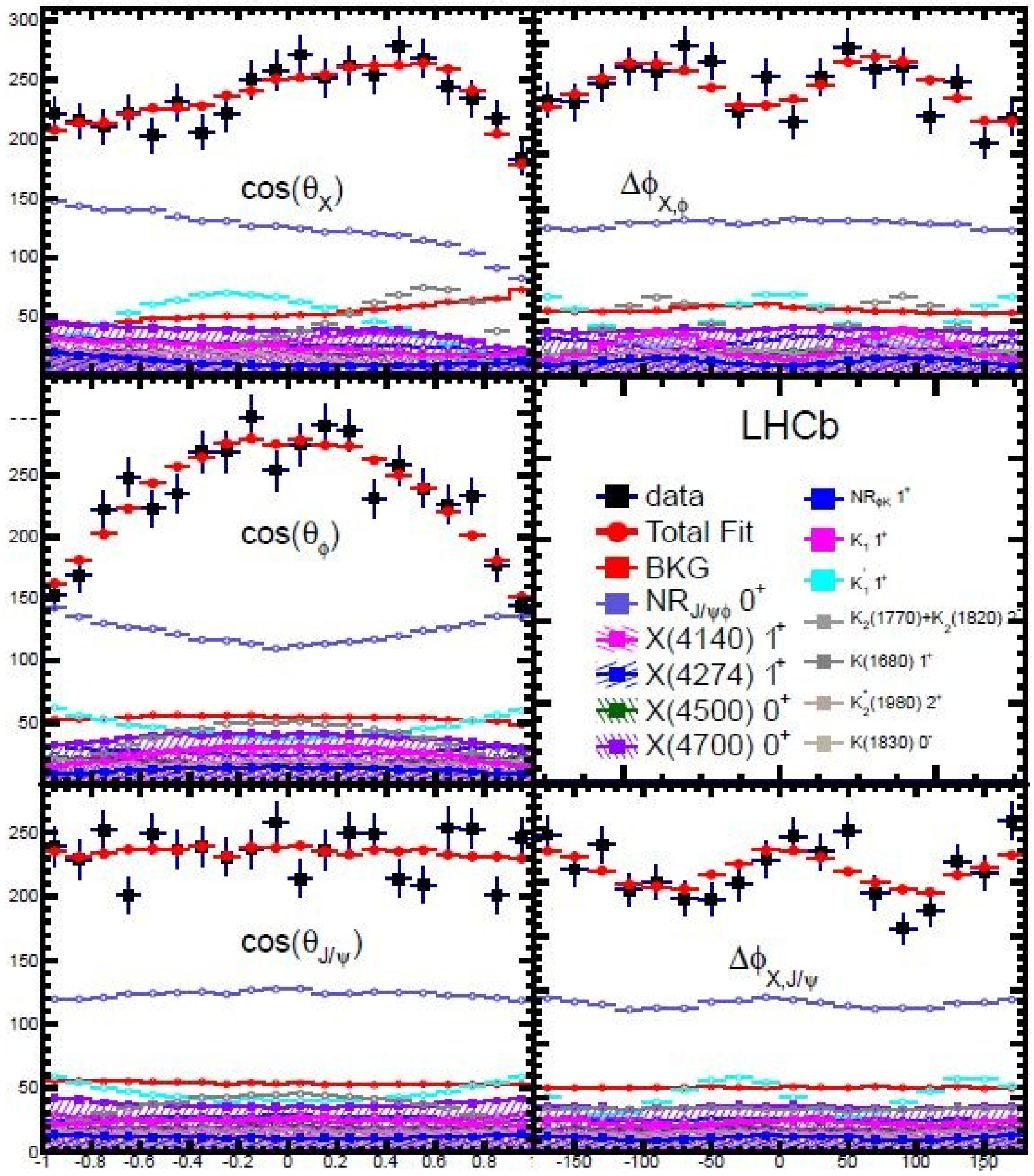
cos(θX)
ΔφX,φ
cos(θφ)
LHCb
data
Total Fit
BKG
NRJ/ψφ 0+
X(4140) 1+
X(4274) 1+
X(4500) 0+
X(4700) 0+
cos(θJ/ψ)
ΔφX,J/ψ

Z angles

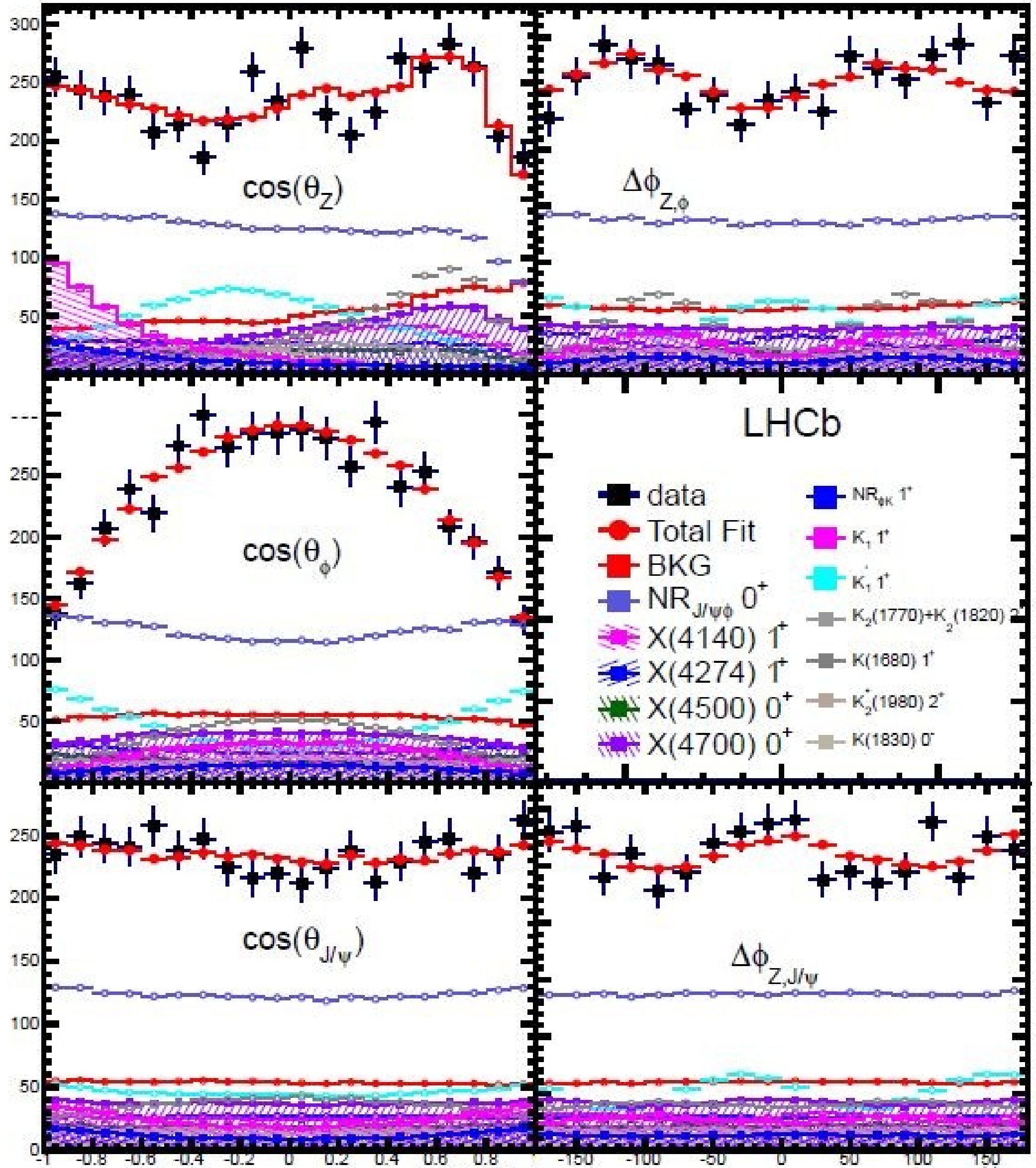
cos(θ_Z)
Δφ_Z,φ
cos(θ_φ)
LHCb
data
Total Fit
BKG
NR_J/ψφ 0+
X(4140) 1+
X(4274) 1+
X(4500) 0+
X(4700) 0+
cos(θ_J/ψ)
Δφ_Z,J/ψ

Fit results in slices of $m_{\phi K}$

$m_{\phi K}$<1750 MeV

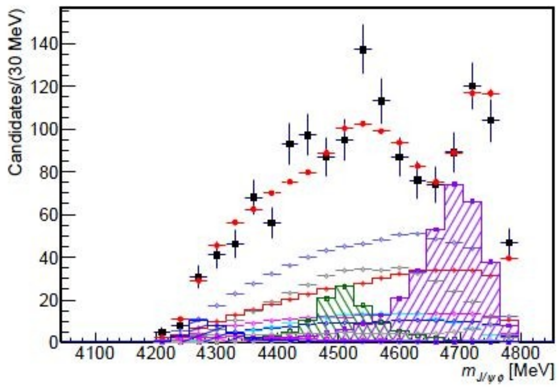

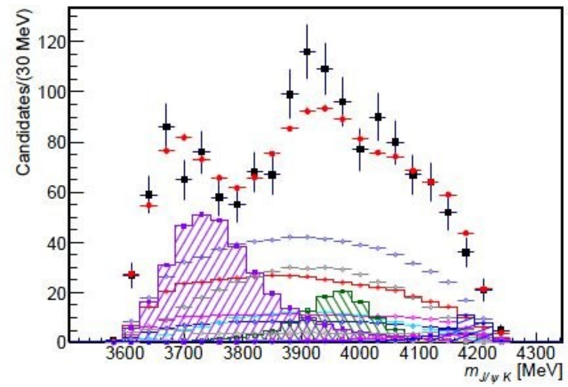

1750≤$m_{\phi K}$≤1950 MeV

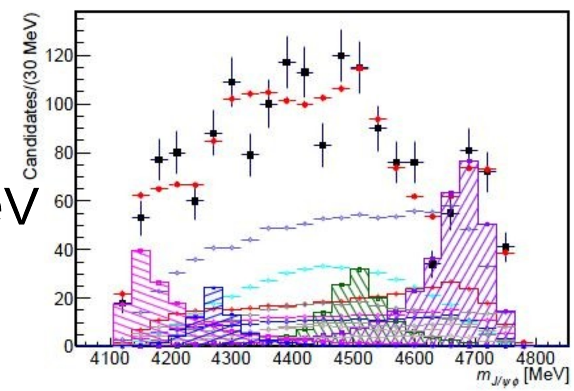

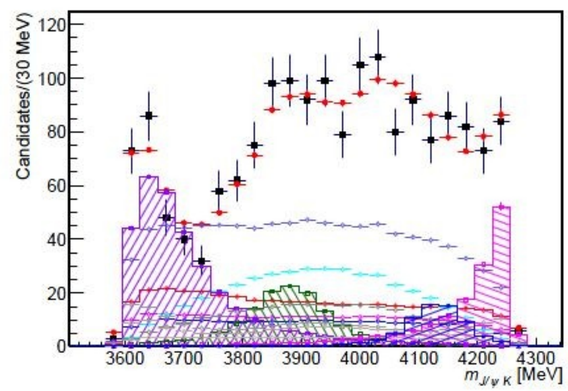

$m_{\phi K}$>1950 MeV

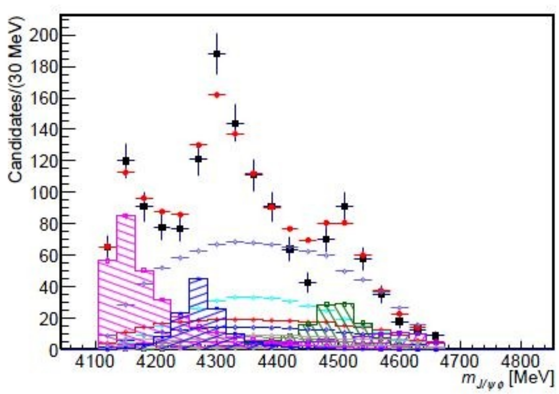

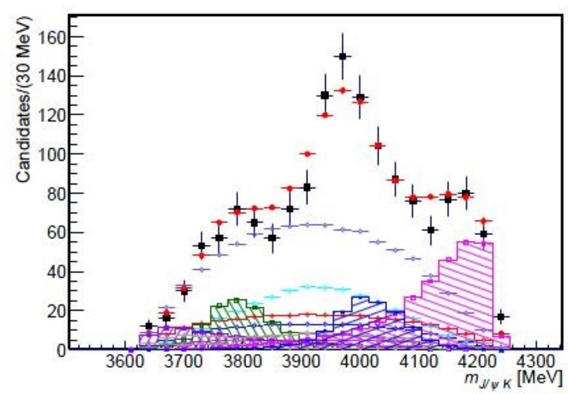

$K^* 1^+$

Contri- bution	sign. or Ref.	M_0 MeV	Γ_0 MeV	Fit results F.F. %
all $K(1^+)$	8.0σ			$42\pm\ 8\,^{+\ 5}_{-\ 9}$
$\mathrm{NR}_{\phi K}$				$16\pm13\,^{+35}_{-\ 6}$
$K(1^+)$	7.6σ	$1793\pm59\,^{+153}_{-101}$	$365\pm157\,^{+138}_{-215}$	$12\pm10\,^{+17}_{-\ 6}$
2^1P_1	[45]	1900		
$K_1(1650)$	[36]	1650 ± 50	$150\pm\ 50$	
$K'(1^+)$	1.9σ	$1968\pm65\,^{+\ 70}_{-172}$	$396\pm170\,^{+174}_{-178}$	$23\pm20\,^{+31}_{-29}$
2^3P_1	[45]	1930		

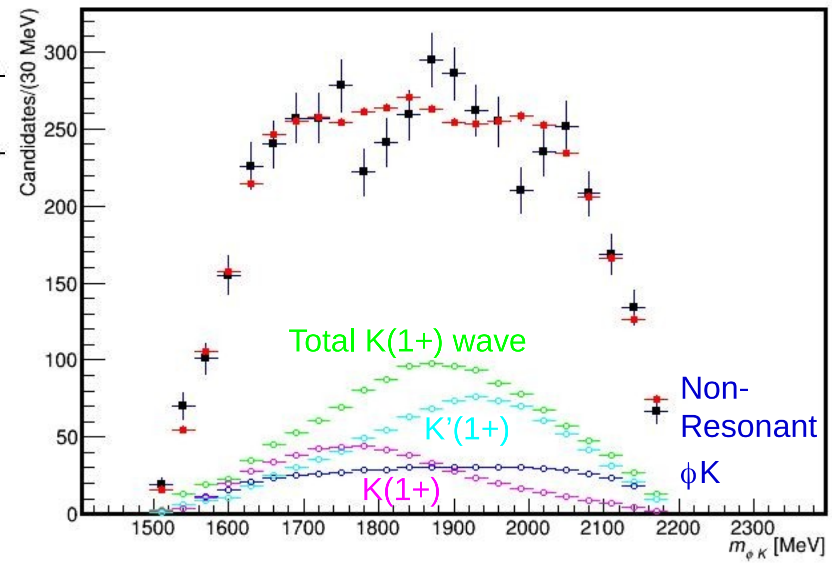

Second state included even with marginal significance because two states are predicted in the quark model (remove it in systematic variation)

Because the 2nd state had borderline significance a 3rd was not tried.

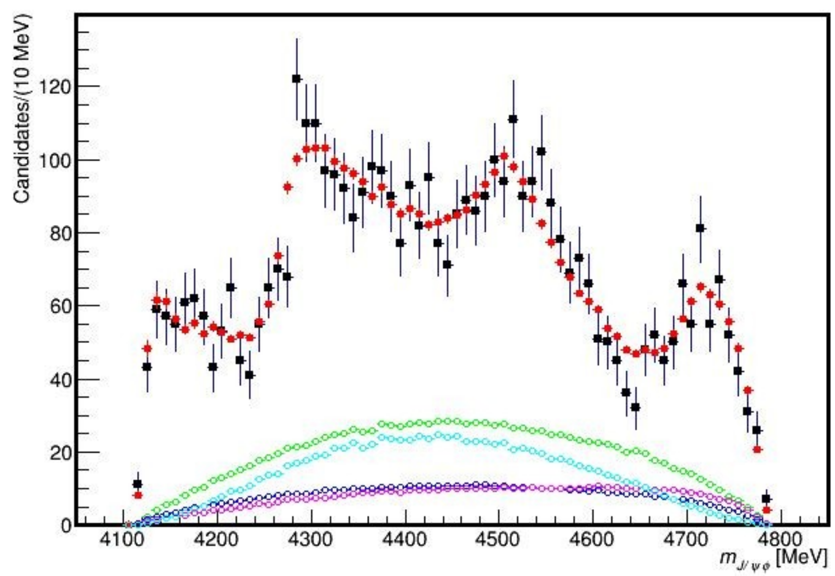

$K^* \ 2^-$

Contribution	sign. or Ref.	M_0 MeV	Γ_0 MeV	F.F. %
			Fit results	
all $K(2^-)$	5.6σ			$11 \pm 3^{+2}_{-5}$
$K(2^-)$	5.0σ	$1777 \pm 35^{+122}_{-77}$	$217 \pm 116^{+221}_{-154}$	
1^1D_2	[45]	1780		
$K_2(1770)$	[36]	1773 ± 8	188 ± 14	
$K'(2^-)$	3.0σ	$1853 \pm 27^{+18}_{-35}$	$167 \pm 58^{+83}_{-72}$	
1^3D_2	[45]	1810		
$K_2(1820)$	[36]	1816 ± 13	276 ± 35	

Excellent agreement with well established PDG $K_2(1770)$ and $K_2(1820)$

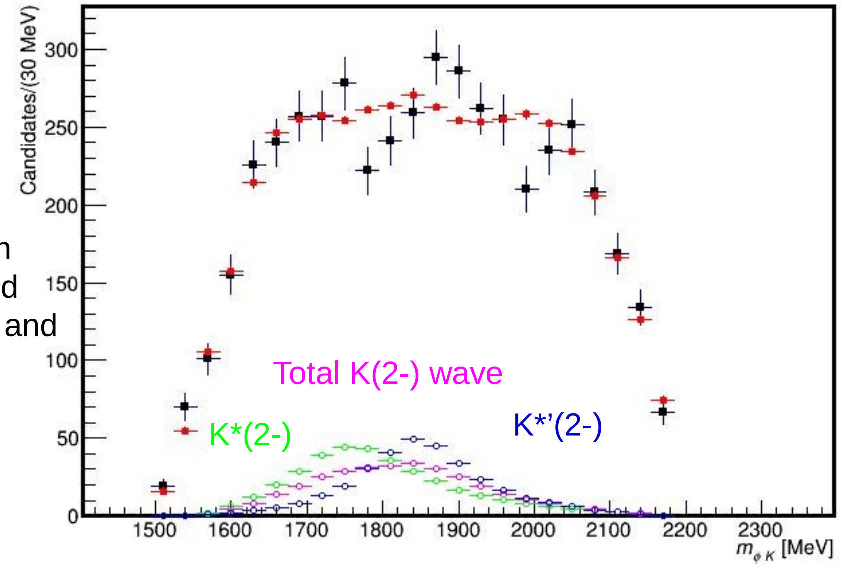

Strong evidence for two 2^- states from prior scattering experiments

Tried one or two additional 2^- states; all significances $<0.2\sigma$

Both states consistent with $K_2(1770)$ and $K_2(1820)$

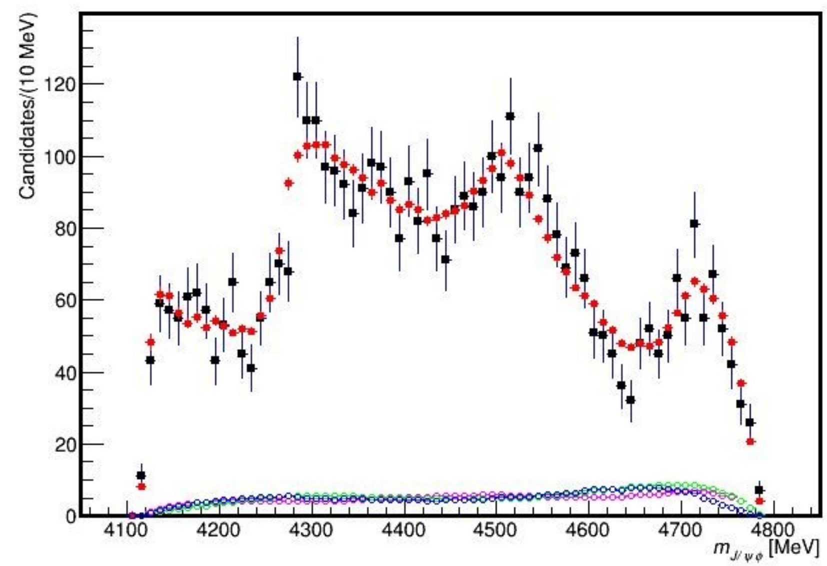

K^* 1^-

Contribution	sign. or Ref.	M_0 MeV	Fit results Γ_0 MeV	F.F. %
$K^*(1^-)$	8.5σ	$1722\pm20\,^{+\,33}_{-109}$	$354\pm\ 75\,^{+140}_{-181}$	$6.7\pm1.9\,^{+3.2}_{-3.9}$
1^3D_1	[45]	1780		
$K^*(1680)$	[36]	1717 ± 27	322 ± 110	

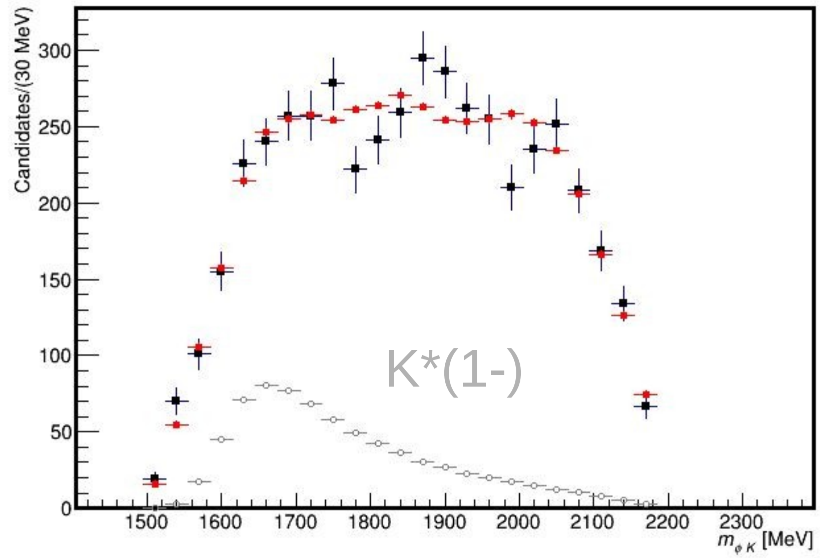

First observation of K*(1680)→ϕK!

Additional 1^- states have a significance of 1.4σ when width is restricted to >100MeV. Higher significance (2.6σ) when allowed to be “exotically” narrow (33±9 MeV)

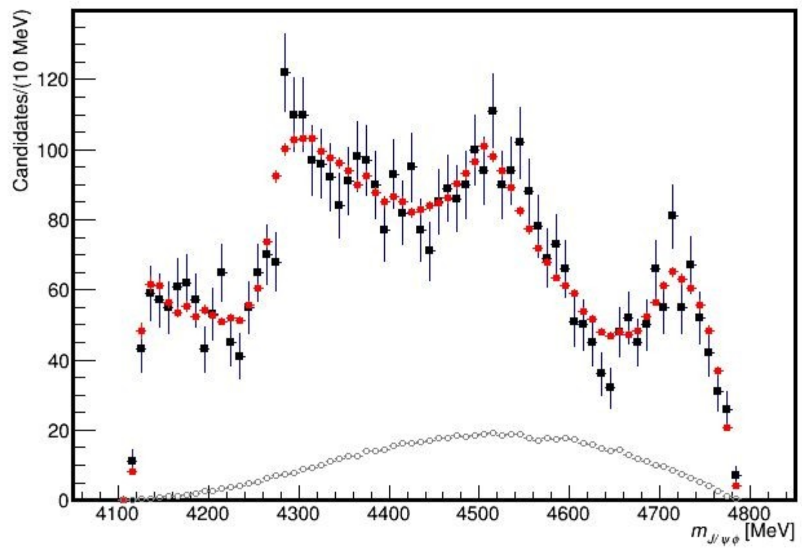

$K^{*}\ 2^{+}$

Contri-bution	sign. or Ref.	Fit results M_0 MeV	Γ_0 MeV	F.F. %
$K^{*}(2^{+})$	5.4σ	$2073 \pm 94\,^{+245}_{-240}$	$678 \pm 311\,^{+1153}_{-559}$	$2.9 \pm 0.8\,^{+1.7}_{-0.7}$
2^3P_2	[45]	1940		
$K_2^{*}(1980)$	[36]	1973 ± 26	373 ± 69	

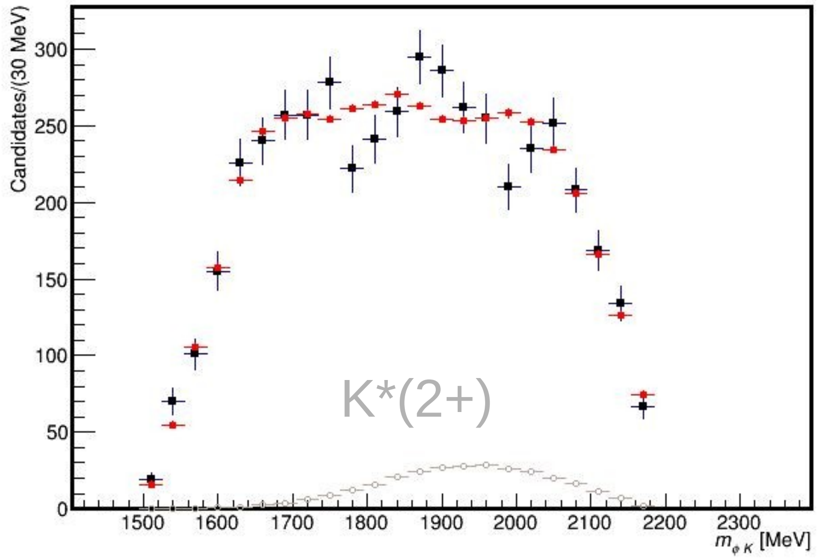

Agrees with $K^{*}_{2}(1980)$ and prior Kp scattering data

Allowing a second 2+ state at 2150 MeV as predicted by Godfrey-Isgur is insignificant ($<1\sigma$) and not included in the default model

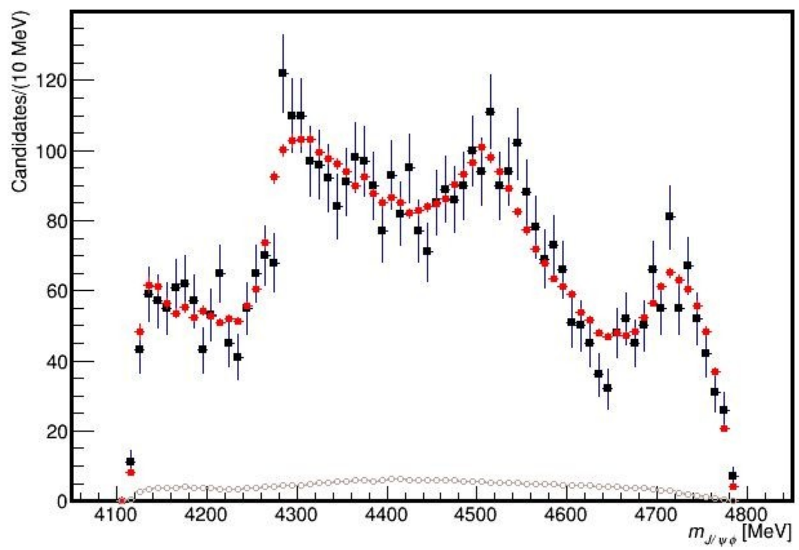

K^{*} 0^{-}

Contribution	sign. or Ref.	M_0 MeV	Fit results Γ_0 MeV	F.F. %
$K(0^-)$	3.5σ	$1874 \pm 43\,^{+59}_{-115}$	$168 \pm 90\,^{+280}_{-104}$	$2.6 \pm 1.1\,^{+2.3}_{-1.8}$
3^1S_0	[45]	2020		
$K(1830)$	[36]	~ 1830	~ 250	

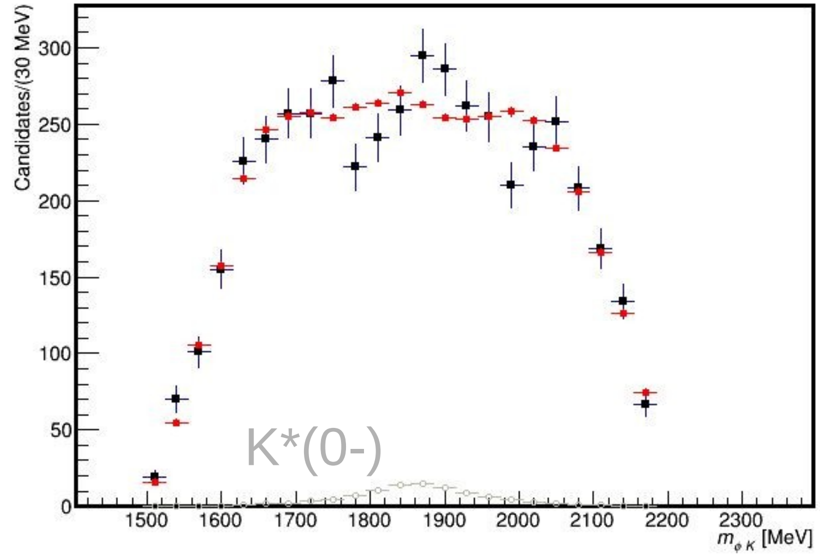

K(0^-) is the smallest contribution by fit fraction

Significantly below Godfrey-Isgur prediction but consistent with the unconfirmed K(1830).

An additional 0^- state is insignificant (0.2σ)

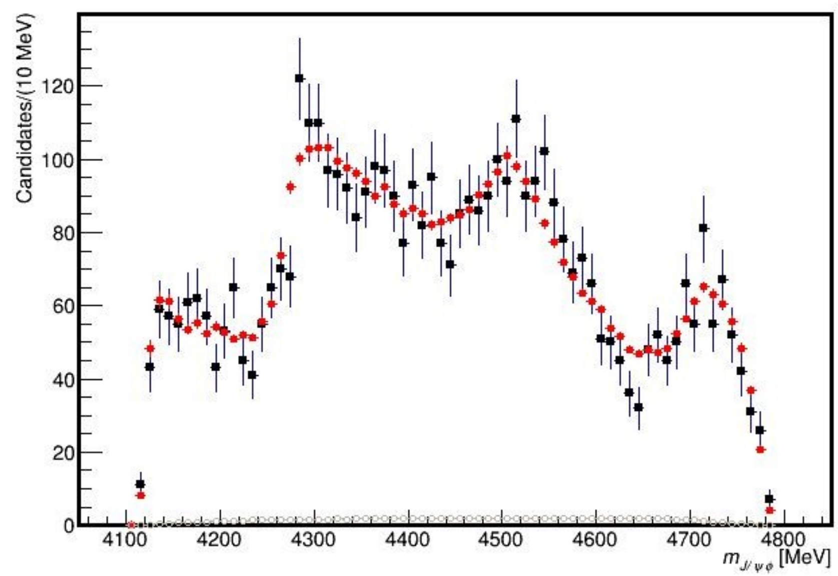

K* results

Our results are given by the red points with error bars

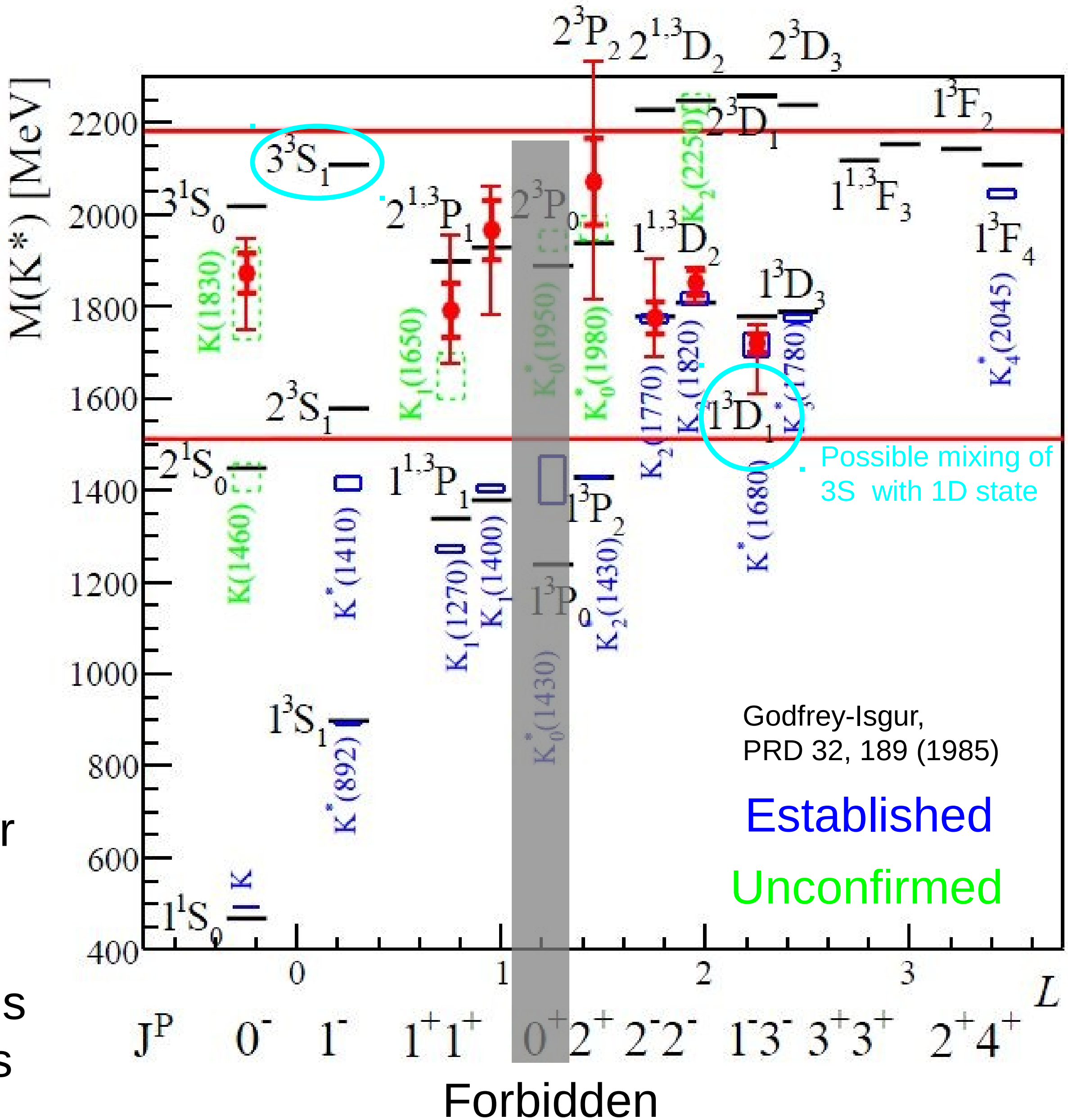

High spin states (3-4) not observed but also expected to be suppressed by orbital angular momentum barrier in B decay

Excellent agreement between our results and both theory and previous experiments

X 1+

Contri-bution	sign. or Ref.	Fit results M_0 MeV	Γ_0 MeV	F.F. %
All $X(1^+)$				$16\pm3\ ^{+\ 6}_{-\ 2}$
$X(4140)$	8.4σ	$4146.5\pm4.5^{+5.2}_{-2.9}$	$83\pm21^{+24}_{-14}$	$13\pm3.2^{+4.8}_{-2.0}$
ave.	Tab. 1	4146.9 ± 2.3	17.8 ± 6.8	
$X(4274)$	6.0σ	$4273.3\pm8.3^{+17.2}_{-\ 3.7}$	$56\pm11^{+9}_{-11}$	$7.1\pm2.5^{+3.6}_{-2.4}$
CDF	[27]	$4274.4^{+8.4}_{-6.7}\pm1.9$	$32^{+22}_{-15}\pm8$	
CMS	[24]	$4313.8\pm5.3\pm7.3$	$38^{+30}_{-15}\pm16$	

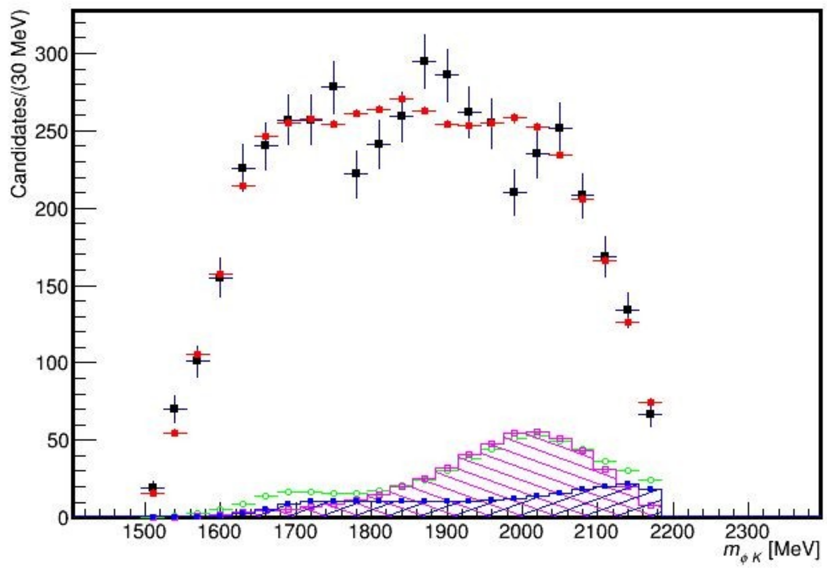

X(4140) agrees with the average of previous measurements though is much broader

X(4274) apparent peaking at ~4300 MeV in data (higher than the pole mass) caused by interferences.

Mass measurement agrees with CDF.

CDF/CMS disagreement may well be explained by interferences and the use of a 1D mass fit

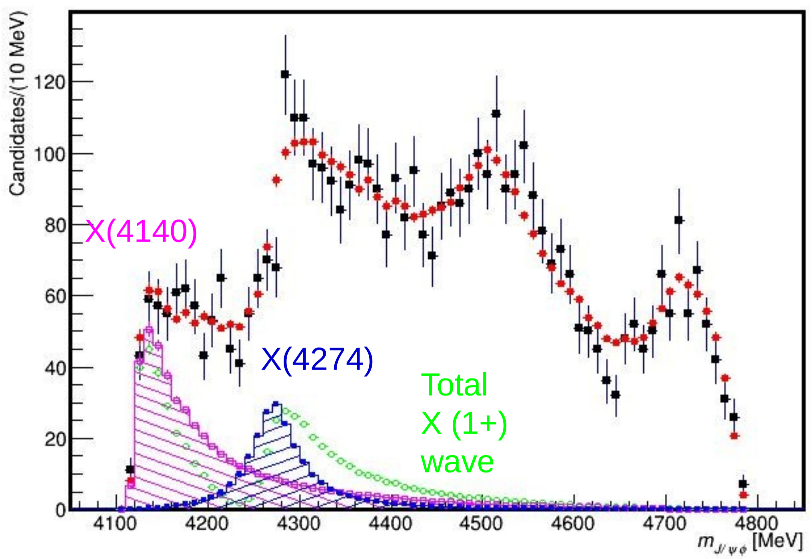

X 0^+

Contri-bution	sign. or Ref.	M_0 MeV	Γ_0 MeV	Fit results F.F. %
All $X(0^+)$				$28 \pm 5^{+7}_{-12}$
$NR_{J/\psi\phi}$	6.4σ			$46 \pm 11^{+17}_{-21}$
$X(4500)$	6.1σ	$4506 \pm 11^{+13}_{-15}$	$92 \pm 21^{+23}_{-20}$	$6.6 \pm 2.4^{+3.5}_{-2.3}$
$X(4700)$	5.6σ	$4704 \pm 10^{+16}_{-24}$	$120 \pm 31^{+43}_{-33}$	$12 \pm 5^{+9}_{-5}$

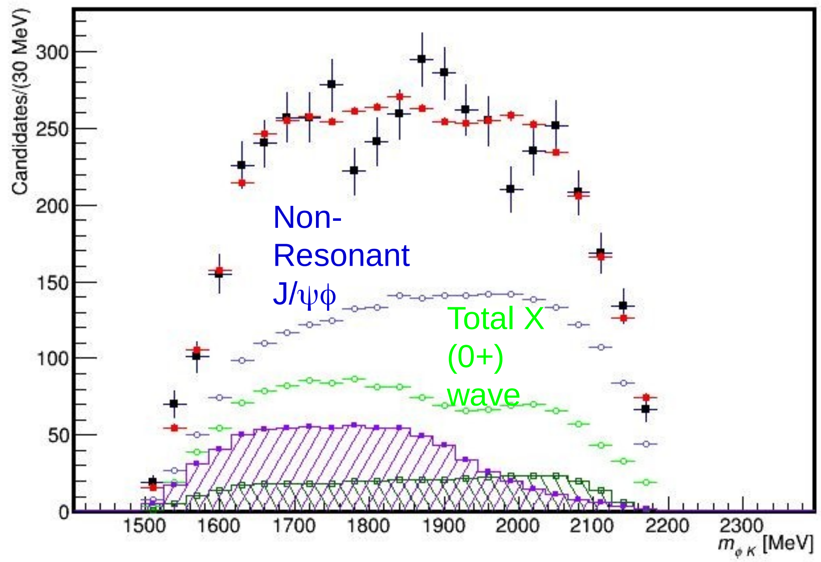

Most striking feature(s) at high mass. The excess is surprising with decreasing phase-space function

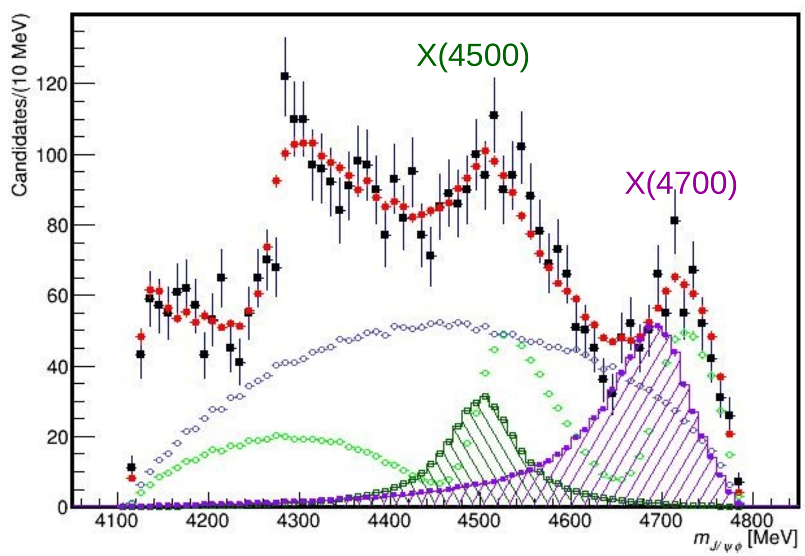

Large NR intensity misleading with strong negative interference

Systematics

sys.	2^-	$K(2^-)$			$K'(2^-)$			1^+	$K(1^+)$			$K'(1^+)$			NR
var.	FF	M_0	Γ_0	FF	M_0	Γ_0	FF	FF	M_0	Γ_0	FF	M_0	Γ_0	FF	FF
K^*	+1.2	+118.1	+194.8	+4.0	+16.2	+53.8	+4.4	+3.9	+150.8	+122.4	+15.6	+49.0	+159.5	+28.5	+34.4
model	-4.1	-22.3	-71.0	-8.6	-14.9	-38.5	-5.5	-7.5	-79.2	-196.2	-6.1	-53.8	-143.2	-27.2	-5.1
L	+0.7	+8.6	+54.1	+3.7	+5.5	+14.0	+3.5	+0.8	+22.3	+20.4	+3.4	+47.5	+37.7	+4.8	+5.0
var.	-1.5	-63.3	-127.9	-9.3	-31.2	-59.5	-8.6	-2.2	-48.6	-70.3	-0.9	-159.9	-72.5	-8.7	-2.2
NR exp.	+0.5	-4.8	-13.5	+0.4	-0.6	+8.6	+1.8	-2.2	-5.9	-3.7	+0.7	-21.4	-45.4	+0.8	+0.3
X cusp	+0.0	+24.6	+42.2	+5.4	-0.8	+10.8	+3.8	+1.8	+4.5	+5.5	+4.4	-12.0	+40.6	+8.4	-0.3
Γ_{tot}	-0.2	+0.8	+38.7	-1.6	-1.9	-12.6	-2.4	+0.6	-29.5	+17.2	+0.9	-0.1	+7.1	-2.3	+2.2
d=1.5	+0.1	+18.2	+67.2	-0.6	+2.7	+6.0	-1.5	+0.7	-17.4	-5.6	-1.0	+8.2	+13.9	-2.1	+1.7
d=5.0	+0.2	-7.2	-25.8	-0.1	-1.0	-0.5	+1.3	-1.5	+12.2	-6.9	+0.5	-8.4	-42.8	-1.0	-1.5
Left s.	+0.1	-4.2	-9.5	-0.2	-1.1	+2.0	+0.9	-1.0	+0.9	+0.2	+1.1	-8.7	-30.2	+0.9	+0.3
Right s.	-0.1	+3.2	+5.0	-0.4	+3.8	+0.1	-1.2	+1.2	-1.3	+12.5	-0.4	+11.6	+36.5	-1.5	-0.1
β	+0.2	-8.1	-35.4	+1.7	-9.3	-6.7	+2.6	-2.7	+28.0	-8.2	+4.0	-23.4	-63.0	+4.8	-0.8
no w^{MC}	-0.8	-0.2	+0.4	-1.1	+0.0	-0.5	-1.5	-0.8	+1.9	+1.2	+0.1	+0.6	+1.8	-0.7	+0.7
ϕ window	-1.0	-25.0	-27.2	-2.6	-1.1	+41.2	-1.4	-2.7	-11.3	-36.5	+0.0	-15.2	-23.1	+6.0	-1.9
Total	+1.5	+122.3	+220.7	+7.7	+17.7	+82.0	+7.2	+4.7	+153.0	+138.0	+16.7	+69.7	+173.5	+31.3	+34.5
sys.	-4.6	-76.5	-154.3	-13.3	-34.7	-72.0	-10.9	-9.2	-100.5	-214.8	-6.3	-172.3	-177.9	-28.8	-6.4
Stat.	2.8	34.9	116.3	11.0	26.6	58.1	11.2	8.1	59.0	157.0	10.3	65.0	170.3	20.4	13.1

Systematics explored included allowing NR to fall off exponentially, varying the K* model, varying L used in each decay (where applicable), using the width from a decay to lighter mesons, variation of the size parameter, fits with only the lower or upper sideband, variation of the ϕ window, no MC reweighting, variation of the **β calculation,** and modeling X(4140) as a cusp (discussed in more detail later)

Systematics continued

sys.	$K^*(1^-)$			$K(0^-)$			$K^*(2^+)$		
var.	M_0	Γ_0	FF	M_0	Γ_0	FF	M_0	Γ_0	FF
K^*	+19.9	+31.4	+2.6	+54.8	+236.9	+1.7	+214.3	+805.2	+1.6
model	-33.1	-141.0	-2.7	-90.2	-96.3	-1.7	-66.9	-223.8	-0.6
L	+14.2	+59.3	+1.8	+12.8	+51.6	+0.7	+52.0	+172.3	+0.3
var.	-17.7	-44.7	-0.2	-44.4	-31.1	-0.2	-19.1	-107.4	-0.3
NR exp.	+3.3	+11.5	+0.2	-22.9	+36.3	+0.4	-13.7	-65.1	+0.0
X cusp	+4.5	+5.5	-1.2	+7.8	+11.4	+0.1	+26.5	+6.1	-0.2
Γ_{tot}	-101.5	-93.1	+0.2	-2.8	-6.2	-0.1	-167.6	-230.0	+0.3
d=1.5	+21.1	+121.7	+0.0	+12.1	+2.5	-0.1	+102.2	+806.2	+0.0
d=5.0	-4.9	-21.0	+0.0	-10.3	+6.3	+0.2	-72.0	-242.5	+0.0
Left s.	+2.7	+7.7	+0.0	-12.6	20.1	+0.2	-17.9	-28.8	+0.2
Right s.	-3.0	+7.7	+0.0	+10.0	-23.5	-0.2	+19.2	+24.7	-0.2
β	+2.2	-4.1	+0.1	-43.0	+32.2	+0.5	-18.5	+1.1	+0.4
no w^{MC}	+0.2	-0.4	+0.1	+1.0	-2.4	-0.4	-0.4	-3.1	-0.2
ϕ window	+0.5	-28.9	-1.8	-33.6	+94.5	+0.9	-97.0	-258.9	+0.2
Total	+32.9	+139.8	+3.2	+59.0	+280.2	+2.3	+245.2	+1152.7	+1.7
sys.	-108.4	-180.7	-3.9	-114.8	-104.1	-1.8	-239.7	-559.0	-0.7
Stat.	19.9	74.7	1.9	43.2	90.4	1.1	94.2	310.6	0.8

Systematics continued

sys.	1^+	$X(4140)$			$X(4274)$			0^+	$X(4500)$			$X(4700)$			NR
var.	FF	M_0	Γ_0	FF	M_0	Γ_0	FF	FF	M_0	Γ_0	FF	M_0	Γ_0	FF	FF
K^*	+2.0	+3.6	+17.1	+2.2	+11.2	+7.9	+1.4	+1.8	+9.3	+13.8	+2.0	+7.5	+38.6	+6.7	+8.0
model	-1.7	-2.6	-11.7	-1.9	-2.5	-8.5	-1.5	-11.0	-8.6	-16.6	-1.7	-18.9	-13.5	-4.8	-16.6
L	+3.2	+2.2	+7.3	+2.1	+10.6	+1.4	+1.0	+0.3	+1.3	+10.8	+1.7	+9.0	+12.4	+1.5	+1.2
var.	+0.0	-1.2	-6.2	-0.5	-0.8	-4.6	-1.2	-4.7	-9.6	-11.2	-1.6	-6.8	-24.9	-0.8	-8.5
NR exp.	+0.4	-0.2	-0.1	+0.4	-0.2	+0.6	+0.8	-1.7	+6.3	+0.3	+0.2	+7.1	-15.7	-1.7	-9.1
X cusp	+2.2			+0.9	+6.4	-5.4	-1.4	-1.2	+0.0	+1.2	+0.2	+1.9	-2.5	0.5	-1.6
Γ_{tot}	-0.6	+0.2	+1.5	-0.4	+3.2	+0.2	-0.3	+0.1	+0.8	-0.1	-0.3	+0.9	-5.8	-0.9	-1.1
d=1.5	-0.9	+1.1	+5.3	-0.5	+2.2	+0.8	-0.4	+0.5	+1.7	+3.2	+0.1	-0.1	+1.7	+0.0	+1.1
d=5.0	+1.1	-0.2	-2.0	+0.6	+0.2	-0.8	+0.3	-0.5	-1.0	-3.1	-0.1	-1.2	-3.2	-0.7	-2.5
Left s.	+0.1	-0.4	-2.0	+0.1	+0.4	-0.8	+0.1	-0.5	-2.4	-2.6	-0.2	-1.5	-3.1	-0.7	-1.2
Right s.	-0.3	+0.3	+2.6	-0.2	-0.6	+1.0	+0.0	+0.5	+3.7	+3.4	+0.4	+1.2	+7.0	+0.8	+1.6
β	+1.2	-0.6	-3.6	+1.2	+1.7	-0.7	+0.9	-2.5	-4.6	-11.1	-0.5	-3.9	-6.1	-1.4	-1.4
no w^{MC}	+1.6	+0.0	+0.0	+0.1	+0.0	+0.0	+1.4	+1.7	+0.0	+0.2	+0.2	+0.1	+0.0	+1.2	+2.7
ϕ window	+2.5	+1.1	+4.7	+2.4	-1.6	+1.4	+1.8	+4.2	-4.3	+7.1	+1.2	-9.3	+5.8	+0.7	+4.7
Total	+5.9	+4.6	+20.7	+4.7	+17.2	+8.4	+3.5	+6.5	+12.0	+20.8	+3.2	+13.9	+42.0	+7.2	+11.0
sys.	-2.1	-2.8	-13.5	-2.0	-3.6	-11.1	-2.4	-6.7	-14.5	-20.4	-2.3	-24.1	-33.3	-5.3	-21.0
Stat.	2.8	4.5	20.7	3.2	8.3	10.9	2.5	5.1	11.1	21.2	2.4	10.1	30.7	4.9	10.7

Spin analysis of X states

J^P/Component	$X(4140)$	$X(4274)$	$X(4500)$	$X(4700)$
0^+	10.3σ	7.8σ	preferred	preferred
0^-	12.5σ	7.0σ	8.1σ	8.2σ
1^+	preferred	preferred	$\mathbf{5.2}\sigma$	$\mathbf{4.9}\sigma$
1^-	10.4σ	$\mathbf{6.4}\sigma$	6.5σ	8.3σ
2^+	$\mathbf{7.6}\sigma$	7.2σ	$\mathbf{5.6}\sigma$	6.8σ
2^-	9.6σ	6.4σ	6.5σ	6.3σ

systematic variation	1^+ $X(4140)$	1^+ $X(4274)$		0^+ $X(4500)$		0^+ $X(4700)$
alternative J^P	2^+	1^-	2^-	1^+	2^+	1^+
default	7.6	6.4	6.4	5.2	5.6	4.9
K_1' L^*_K+2	12.2	6.2	7.4	5.4	6.5	5.1
$K_2(1770)$ L^*_K+2	**5.7**	6.0	**5.8**	5.2	4.9	4.5
$K_3^*(1780)$ (3^-)	6.2	6.6	6.3	4.9	5.1	**4.5**
NR exp	7.5	6.5	6.1	8.9	5.8	4.7
$K^{*\prime}(1^-)$	6.8	6.1	**5.8**	5.8	6.2	4.7
$K^{'''}(2^-)$	6.9	6.7	6.2	**4.0**	6.6	4.8

- On the left is the significance of the preferred quantum numbers over the other hypothesis in the default model
- On the right are the significance of the preferred quantum numbers over the next closest quantum number(s) (as determined by the preferences of the default model) for a subset of systematic studies that yielded the largest changes in X parameters.

- **Quantum numbers of X(4140) determined for the first time as $J^{PC}=1^{++}$ by >5.7σ**
- **Quantum numbers of X(4274) determined for the first time as $J^{PC}=1^{++}$ by >5.8σ**

K* polarizations

- Given the advancements in K* spectroscopy that have been made in this analysis it is of some interest to compute the longitudinal and transverse polarizations for the K* states included in the default model. This is done through the equations below with results given on the following page with the other numerical results. Numerical results for the polarizations on the next slide are given with statistical errors.

$$f_L = \frac{\left|A_{\lambda=0}^{B\to J/\psi\, K^*}\right|^2}{\left|A_{\lambda=-1}^{B\to J/\psi\, K^*}\right|^2 + \left|A_{\lambda=0}^{B\to J/\psi\, K^*}\right|^2 + \left|A_{\lambda=+1}^{B\to J/\psi\, K^*}\right|^2},$$

$$A_{\perp}^{B\to J/\psi\, K^*} = \frac{A_{\lambda=+1}^{B\to J/\psi\, K^*} - A_{\lambda=-1}^{B\to J/\psi\, K^*}}{\sqrt{2}},$$

$$f_{\perp} = \frac{\left|A_{\perp}^{B\to J/\psi\, K^*}\right|^2}{\left|A_{\lambda=-1}^{B\to J/\psi\, K^*}\right|^2 + \left|A_{\lambda=0}^{B\to J/\psi\, K^*}\right|^2 + \left|A_{\lambda=+1}^{B\to J/\psi\, K^*}\right|^2}.$$

All results put together

Contri-bution	sign. or Ref.	Fit results M_0 MeV	Γ_0 MeV	F.F. %	f_L	$f_\perp$
all $K(1^+)$	8.0σ			$42\pm 8^{+5}_{-9}$		
$NR_{\phi K}$				$16\pm13^{+35}_{-6}$	0.52 ± 0.29	0.21 ± 0.16
$K(1^+)$	7.6σ	$1793\pm59^{+153}_{-101}$	$365\pm157^{+138}_{-215}$	$12\pm10^{+17}_{-6}$	0.24 ± 0.21	0.37 ± 0.17
2^1P_1	[45]	1900				
$K_1(1650)$	[36]	1650 ± 50	150 ± 50			
$K'(1^+)$	1.9σ	$1968\pm65^{+70}_{-172}$	$396\pm170^{+174}_{-178}$	$23\pm20^{+31}_{-29}$	0.04 ± 0.08	0.49 ± 0.10
2^3P_1	[45]	1930				
all $K(2^-)$	5.6σ			$11\pm 3^{+2}_{-5}$		
$K(2^-)$	5.0σ	$1777\pm35^{+122}_{-77}$	$217\pm116^{+221}_{-154}$		0.64 ± 0.11	0.13 ± 0.13
1^1D_2	[45]	1780				
$K_2(1770)$	[36]	1773 ± 8	188 ± 14			
$K'(2^-)$	3.0σ	$1853\pm27^{+18}_{-35}$	$167\pm 58^{+83}_{-72}$		0.53 ± 0.14	0.04 ± 0.08
1^3D_2	[45]	1810				
$K_2(1820)$	[36]	1816 ± 13	276 ± 35			
$K^*(1^-)$	8.5σ	$1722\pm20^{+33}_{-109}$	$354\pm 75^{+140}_{-181}$	$6.7\pm1.9^{+3.2}_{-3.9}$	0.82 ± 0.04	0.03 ± 0.03
1^3D_1	[45]	1780				
$K^*(1680)$	[36]	1717 ± 27	322 ± 110			
$K^*(2^+)$	5.4σ	$2073\pm94^{+245}_{-240}$	$678\pm311^{+1153}_{-559}$	$2.9\pm0.8^{+1.7}_{-0.7}$	0.15 ± 0.06	0.79 ± 0.08
2^3P_2	[45]	1940				
$K_2^*(1980)$	[36]	1973 ± 26	373 ± 69			
$K(0^-)$	3.5σ	$1874\pm43^{+59}_{-115}$	$168\pm 90^{+280}_{-104}$	$2.6\pm1.1^{+2.3}_{-1.8}$	1.0	
3^1S_0	[45]	2020				
$K(1830)$	[36]	~ 1830	~ 250			
All $X(1^+)$				$16\pm3^{+6}_{-2}$		
$X(4140)$	8.4σ	$4146.5\pm4.5^{+4.6}_{-2.8}$	$83\pm21^{+21}_{-14}$	$13\pm3.2^{+4.8}_{-2.0}$		
ave.	Table [1]	4146.9 ± 2.3	17.8 ± 6.8			
$X(4274)$	6.0σ	$4273.3\pm8.3^{+17.2}_{-3.6}$	$56\pm11^{+8}_{-11}$	$7.1\pm2.5^{+3.5}_{-2.4}$		
CDF	[27]	$4274.4^{+8.4}_{-6.7}\pm1.9$	$32^{+22}_{-15}\pm8$			
CMS	[24]	$4313.8\pm5.3\pm7.3$	$38^{+30}_{-15}\pm16$			
All $X(0^+)$				$28\pm 5^{+7}_{-7}$		
$NR_{J/\psi\phi}$	6.4σ			$46\pm11^{+11}_{-21}$		
$X(4500)$	6.1σ	$4506\pm11^{+12}_{-15}$	$92\pm21^{+21}_{-20}$	$6.6\pm2.4^{+3.5}_{-2.3}$		
$X(4700)$	5.6σ	$4704\pm10^{+14}_{-24}$	$120\pm31^{+42}_{-33}$	$12\pm 5^{+9}_{-5}$		

$$f_L = \frac{\left|A^{B\to J/\psi K^*}_{\lambda=0}\right|^2}{\left|A^{B\to J/\psi K^*}_{\lambda=-1}\right|^2 + \left|A^{B\to J/\psi K^*}_{\lambda=0}\right|^2 + \left|A^{B\to J/\psi K^*}_{\lambda=+1}\right|^2},$$

$$A_\perp^{B\to J/\psi K^*} = \frac{A^{B\to J/\psi K^*}_{\lambda=+1} - A^{B\to J/\psi K^*}_{\lambda=-1}}{\sqrt{2}},$$

$$f_\perp = \frac{\left|A^{B\to J/\psi K^*}_{\perp}\right|^2}{\left|A^{B\to J/\psi K^*}_{\lambda=-1}\right|^2 + \left|A^{B\to J/\psi K^*}_{\lambda=0}\right|^2 + \left|A^{B\to J/\psi K^*}_{\lambda=+1}\right|^2}.$$

X exotics as cusps

Isobar Model

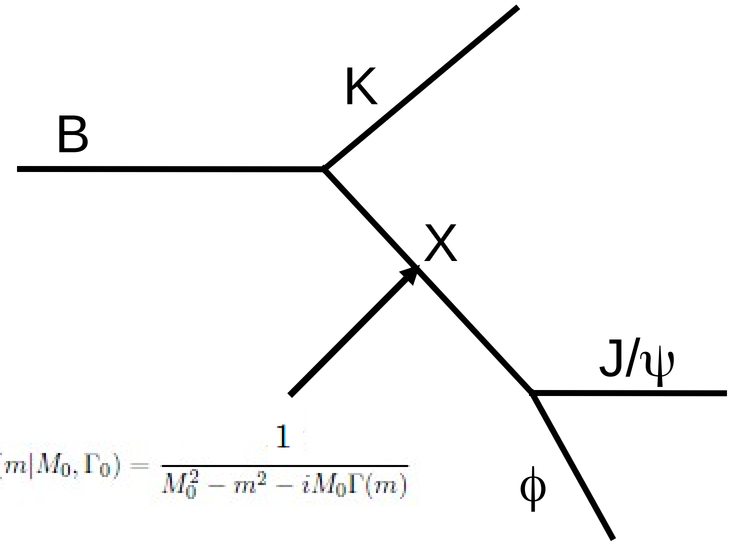

$$BW(m|M_0,\Gamma_0) = \frac{1}{M_0^2 - m^2 - iM_0\Gamma(m)}$$

Cusps

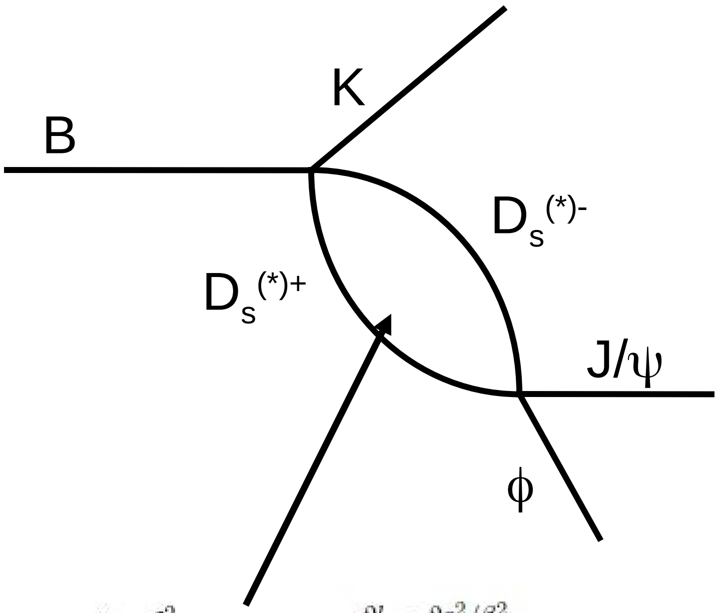

$$\Pi(m) = \int \frac{d^3q}{(2\pi)^3} \frac{q^{2l}\, e^{-2q^2/\beta_{AB}^2}}{m - M_A - M_B - \frac{q^2}{2\mu_{AB}} + i\,\epsilon}$$

Swanson model Argand diagram

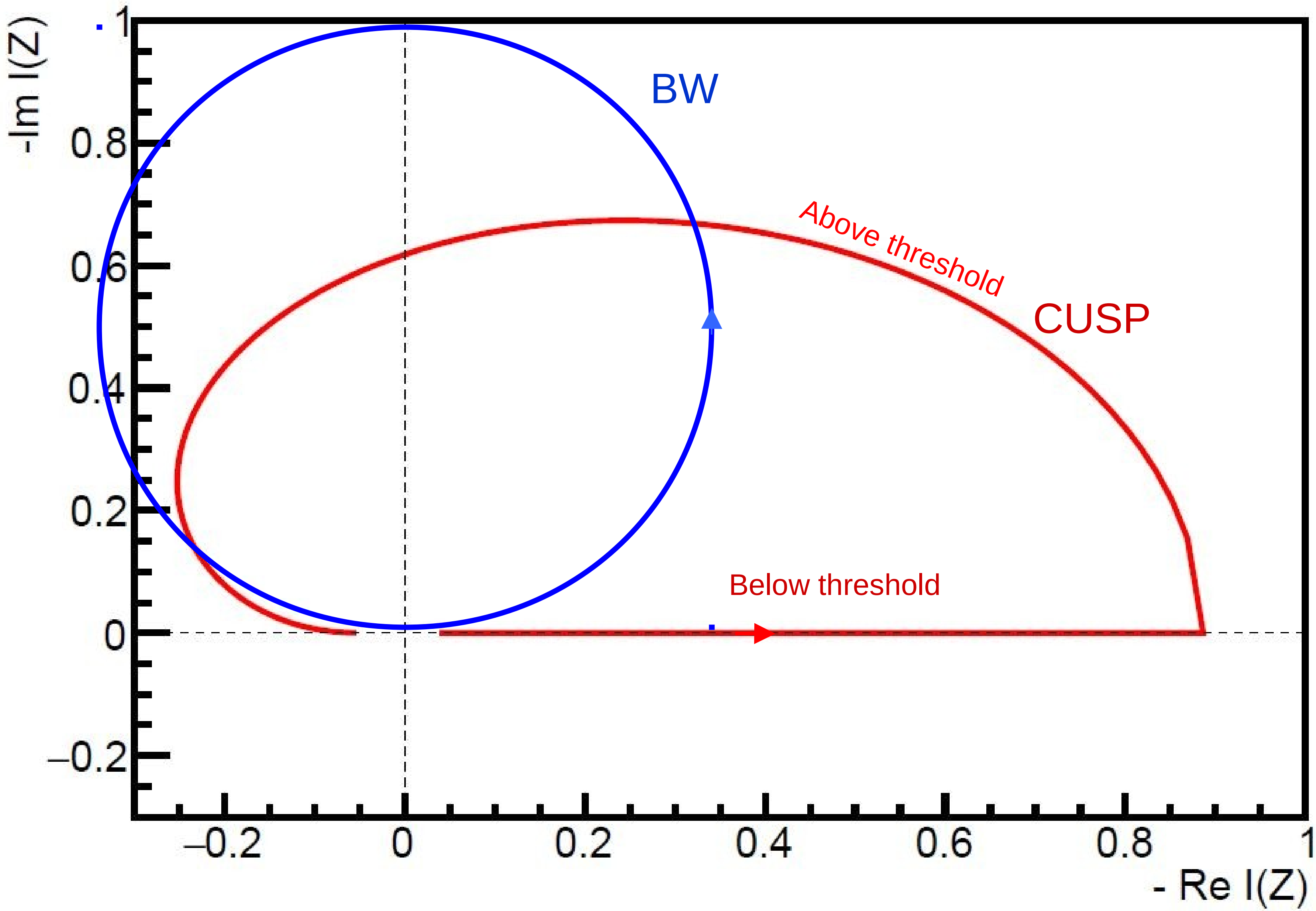

Cusps

- Additional models were tried including a fairly simple model of a coupled channel cusp by Swanson

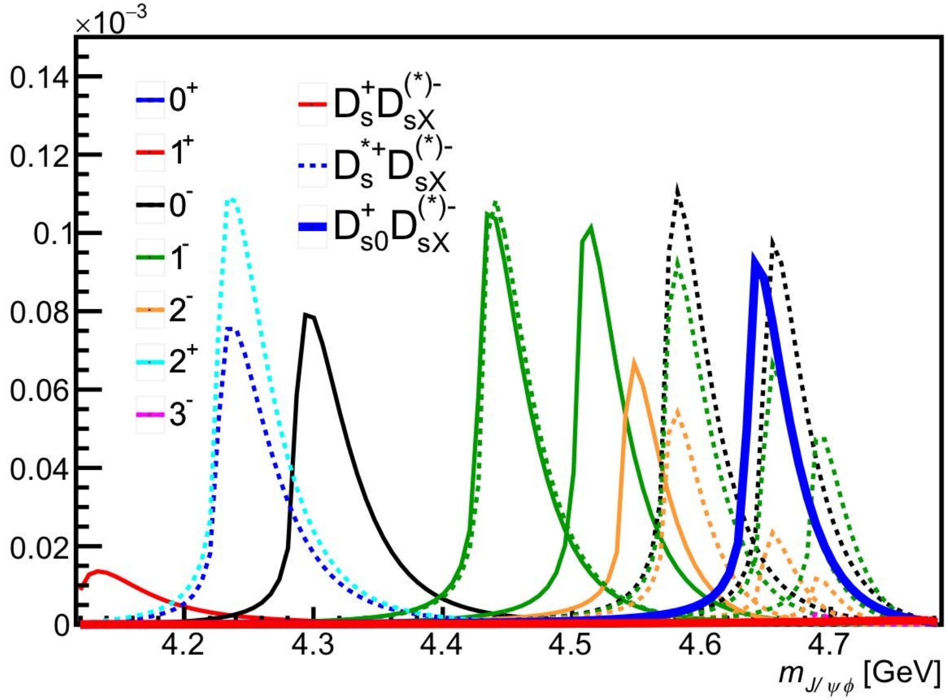

- Various cusps from the DsDs sector were tried to explain the various exotic peaks as non-exotic cusps, or their interferences

X(4140) as a cusp

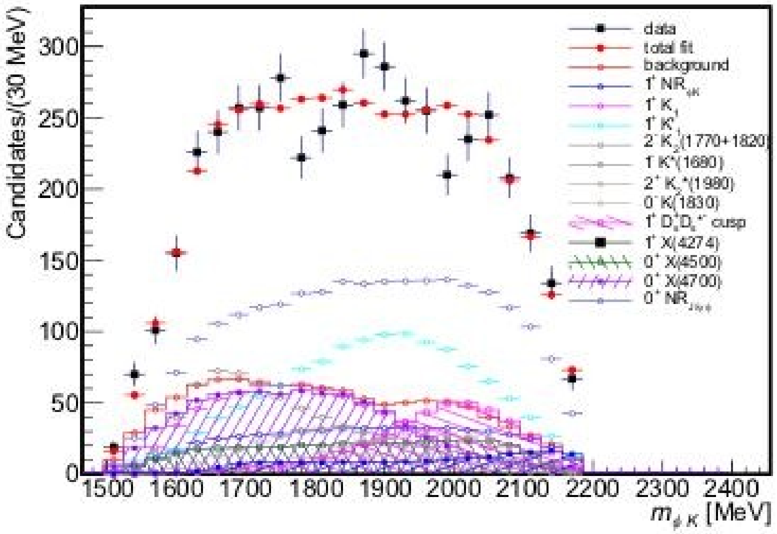

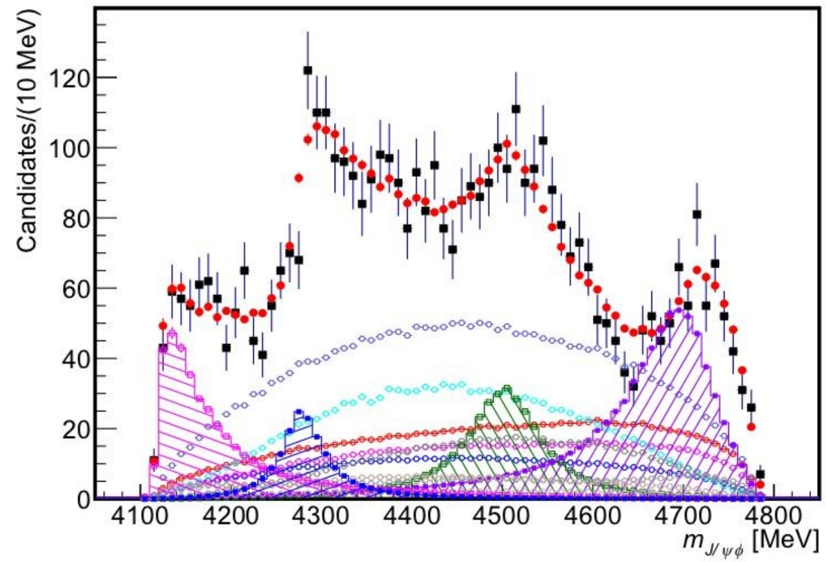

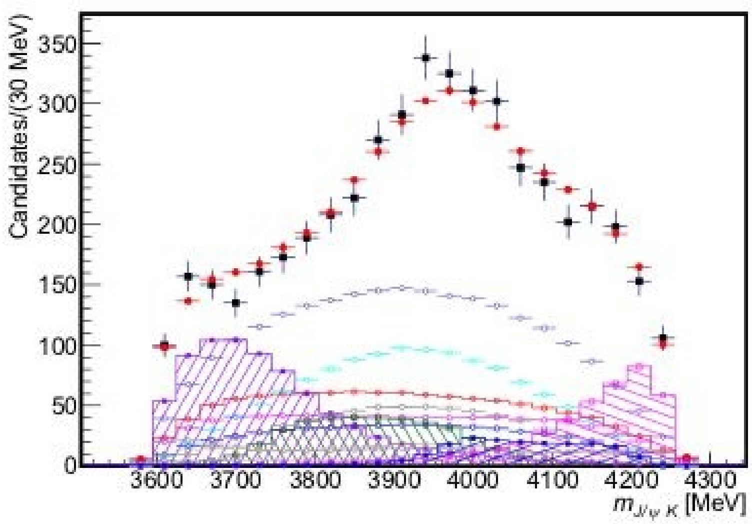

With X(4140) represented by a $J^p=1^+$ $D_s^+D_s^{*-}$ cusp we find the fit to be slightly better than the default model with $\Delta(-2*\text{Ln}(L))= 3^2$ (favoring the cusp model)

X(4140) and X(4274) as cusps

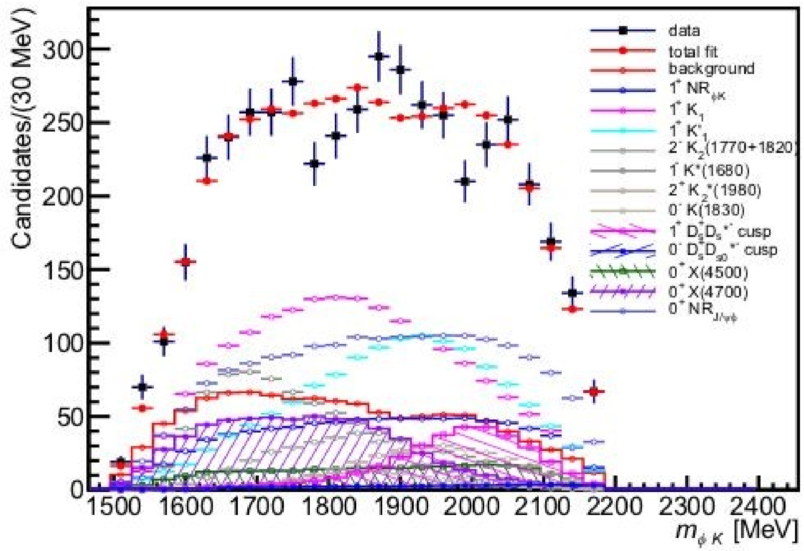

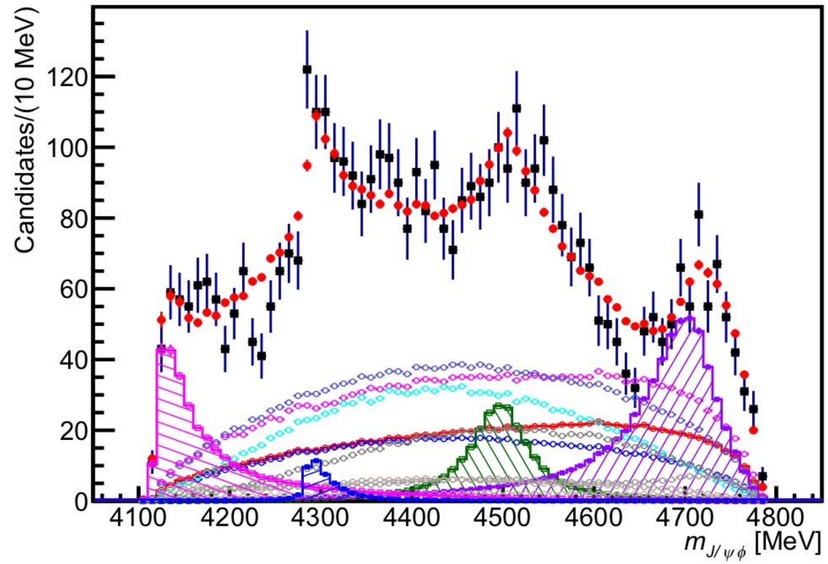

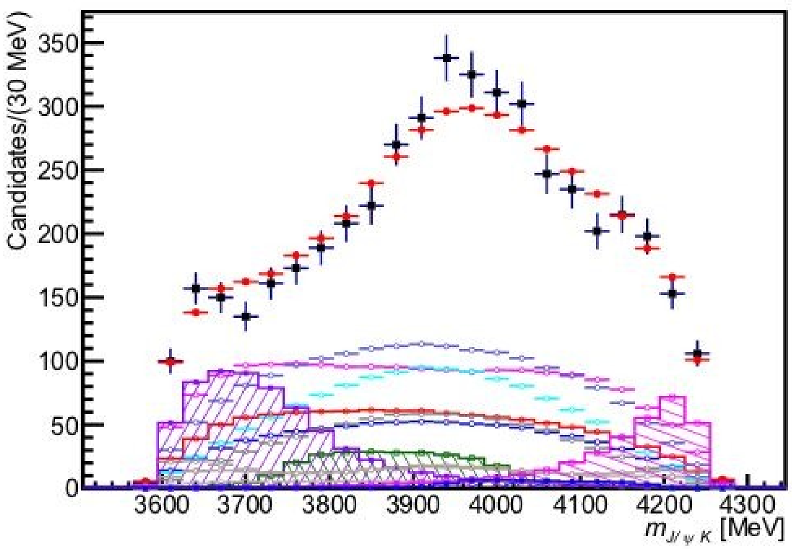

- Attempts to replace more than X(4140) with cusps were performed but did not produce better fits
- This fit, in which, X(4140) is replaced with a 1^{++} $D_s^+D_s^{*-}$ cusp **and X(4274) is replaced with a 0^{-+} $D_s^+D_{s0}^{*-}$ cusp** is worse than the default fit by $\Delta(-2*\mathrm{Ln}(L))= 5.9^2$ (favoring the BW model)

Theoretical interpretations

Molecular models

- The determination of the quantum numbers of X(4140) as $J^{PC}=1^{++}$ rules out many interpretations. Namely, 0^{++} or 2^{++} $D_s^*\bar{D}_s^*$ molecules. The large width is also not expected for true molecular bound states.
- However, X(4140) may be a 1^{++} $D_sD_s^*$ cusp (form of rescattering)

Hybrid models

- Hybrid charmonium states would have $J^{PC}=1^{-+}$. Thus they are also ruled out.

Tetraquark models

- There are many tetraquark models which predict states with $J^{PC}=0^{-+}$, 1^{-+} or 0^{++}, 2^{++}; these can be ruled out.
- A tetraquark model implemented by Stancu correctly assigns 1^{++} to X(4140) and predicts a second 1^{++} state at a mass not much higher than X(4274)
- A Lattice calculation by Padmanth et al, based on a diquark tetraquark model, found no evidence for a 1^{++} tetraquark below 4.2 GeV

Results summary for K*

- Little in the way of apparent features in the mass spectrum but angular distributions lead to a robust tapestry of K* states.
- **1^+ partial wave**: dominant with at least one resonance at 7.6σ significance.
- **2^- partial wave**: comprised of 2 resonances in good agreement with well established $K_2(1770)$ and $K_2(1820)$
- **1^- partial wave**: First observation of $K^*(1680) \to \phi K$
- **2^+ partial wave**: with 5.4σ evidence for a broad resonance consistent with $K_2^*(1980)$
- **0^- partial wave**: 3.5σ evidence for the earlier observed K(1830).
- First proper error analysis of many high mass K* states (previous results often don't have any systematic analysis)

- **K* results consistent with expectations and prior measurements**

X results summary

X states:	sig.	Mass	Width	FF
Possible cusp $X(4140)$	8.4σ	$4146.5 \pm 4.5^{+5.2}_{-2.9}$	$83 \pm 21^{+24}_{-14}$	$13 \pm 3.2^{+4.8}_{-2.0}$
Determined to be 1^{++} for the first time				
$X(4274)$	6.0σ	$4273.3 \pm 8.3^{+17.2}_{-\ 3.7}$	$56 \pm 11^{+9}_{-11}$	$7.1 \pm 2.5^{+3.6}_{-2.4}$
Determined to be 1^{++} for the first time				
NEW! (0^{++}) $X(4500)$	6.1σ	$4506 \pm 11^{+13}_{-15}$	$92 \pm 21^{+23}_{-20}$	$6.6 \pm 2.4^{+3.5}_{-2.3}$
(0^{++}) $X(4700)$	5.6σ	$4704 \pm 10^{+16}_{-24}$	$120 \pm 31^{+43}_{-33}$	$12 \pm\ 5^{+\ 9}_{-\ 5}$

The high J/ψϕ mass region has been investigated for the first time with good sensitivity. No theoretical models, except for Wang et al that predicted a 0^{++} state at 4.48±0.17 GeV, exist for these high mass features

The complexity of the J/ψϕ model and the failure of existing models to describe all of the features of $m_{J/\psi\phi}$ suggest the data may have a complicated origin. Hopefully this work will stimulate discussion of amplitude parameterizations to be tried in the future in order to clarify the nature of the observed J/ψϕ structures

BACKUP SLIDES

Dalitz plots

- All plots are efficiency corrected and background subtracted with density of points proportional to bin content